This patient survived for 27 months after the onset of clinical symptoms, which exceeds the mean survival period in national surveillance studies (12.7 months; range, 1–61) in Japan (10). PPS treatment did not alter the clinical course from the initial akinetic mute state. Thus, her prolonged survival might be partially attributable to both good nursing care and active medical interventions for malnutrition and pneumonia. The present study is a preliminary case study in a sCJD patient with pentosan therapy, and placebo-controlled study with PPS infusion will be needed in the future.

Prion protein deposition was not dramatically different between the hemisphere implanted with the catheter and the opposite hemisphere, unlike data reported in a rodent model (1). Here, the treatment started at an advanced clinical stage that may have already involved extensive PrP deposition, whereas treatment in the rodent model started before PrP deposition. In addition, difference of cerebrospinal fluid flow dynamics in the brain ventricular system between rodents and humans might contribute to the discrepancy. However, we found lower levels of abnormal protease-resistant PrP here than in other untreated sCJD patients, suggesting that PPS infusion might suppress the accumulation of abnormal PrP in the brain.

This speculation requires to be further evaluated, because there are possibilities that the gap of abnormal PrP levels between the patient and the control subjects might be attributable to the difference in disease durations or brain sampling regions, or to the regional variety of abnormal PrP deposition. These possibilities could not be evaluated in the present study because of limited sample availability.

Acknowledgements

The intraventricular PPS trial in this case was supported by a grant from the Japanese Ministry of Health, Labor and Welfare (H19-nanji-ippan-006).

References

1. Doh-ura K, Ishikawa K, Murakami-Kubo I et al. Treatment of transmissible spongiform encephalopathy by intraventricular drug infusion of animal models. J Virol 2004;**78**: 4999–5006.
2. Parry A, Baker I, Stacey R, Wimalaratna S. Long term survival in a patient with variant Creutzfeldt–Jakob disease treated with intraventricular pentosan polysulphate. J. Neurol Neurosurg Psychiat 2007;**78**:733–4.
3. Todd NV, Morrow J, Doh-ura K et al. Cerebroventricular infusion of pentosan polysulphate in human variant Creutzfeldt–Jakob disease. J Infect 2005;**50**:394–6.
4. Whittle IR, Knight RSG, Will RG. Unsuccessful intraventricular pentosan polysulphate treatment of variant Creutzfeldt–Jakob disease. Acta Neurochir (Wien) 2006;**148**: 677–9.
5. Rainov NG, Tsuboi Y, Krolak-Salmon P, Vighetto A, Doh-Ura K. Experimental treatments for human transmissible spongiform encephalopathies: is there a role for pentosan polysulfate? Expert Opin Biol Ther 2007;**7**:713–26.
6. Bone I, Belton L, Walker AS, Darbyshire J. Intraventricular pentosan polysulphate in human prion diseases: an observational study in the UK. Eur J Neurol 2008;**15**: 458–64.
7. Hizume M, Kobayashi A, Teruya K et al. Human Prion Protein (PrP) 219K is converted to PrPSc but shows heterozygous inhibition in variant Creutzfeldt–Jakob disease infection. J Biol Chem 2009;**284**:3603–9.
8. Farquhar C, Dickinson A, Bruce M. Prophylactic potential of pentosan polysulphate in transmissible spongiform encephalopathies. Lancet 1999;**353**:117.
9. Ladogana A, Casaccia P, Ingrosso L et al. Sulphate polyanions prolong the incubation period of scrapie-infected hamsters. J Gen Virol 1992;**73**:661–5.
10. Mizusawa H. Prion disease – an overview. Neurol Med 2005;**63**:409–16.

Copyeditor: Jamaica Polintan

J Neuropathol Exp Neurol
Copyright © 2010 by the American Association of Neuropathologists, Inc.

Vol. 69, No. 7
July 2010
pp. 00–00

ORIGINAL ARTICLE

Neuropathological Asymmetry in Argyrophilic Grain Disease

Tadashi Adachi, MD, Yuko Saito, MD, PhD, Hiroyuki Hatsuta, MD, Sayaka Funabe, MD, Aya M. Tokumaru, MD, PhD, Kenji Ishii, MD, Tomio Arai, MD, PhD, Motoji Sawabe, MD, PhD, Kazutomi Kanemaru, MD, PhD, Akinori Miyashita, PhD, Ryozo Kuwano, MD, PhD, Kenji Nakashima, MD, PhD, and Shigeo Murayama, MD, PhD

Abstract

The presence of argyrophilic grains in the neuropil is associated with a form of dementia. We investigated morphological asymmetry in 653 consecutive autopsy patients from a general geriatric hospital (age [mean ± SD] = 81.1 ± 8.9 years), focusing on those from patients with advanced argyrophilic grain disease. Paraffin sections of the bilateral posterior hippocampi were immunostained with anti–phosphorylated tau and anti–4-repeat tau antibodies and by the Gallyas-Braak method. In a side-to-side comparison, asymmetry was defined when either the extent or the density of argyrophilic grains was different. Of the 653 subjects, 65 (10%) had Stage 3 argyrophilic grain disease, and 59 (90.8%) showed histopathological asymmetry. Antemortem computed tomographic images (n = 24), magnetic resonance imaging scans (n = 8), and combined computed tomographic and magnetic resonance images (n = 15) were available; images from 20 of the 47 subjects showed asymmetry that correlated with the histopathological asymmetry. Cerebral cortical asymmetry consistent with the histopathology was also visible in *N*-isopropyl-^{123}I-*p*-iodoamphetamine single photon emission computed tomographic images from 6 patients and ^{18}F-labeled fluorodeoxyglucose positron emission tomographic images from 2 patients. Thus, asymmetric involvement of the medial temporal lobe in patients with advanced argyrophilic grain disease may represent a diagnostic feature and contribute to distinguishing dementia with grains from Alzheimer disease.

Key Words: Alzheimer disease, Argyrophilic grain, Asymmetry, Dementia, MRI, Neuroimaging, tau Protein.

From the Department of Neuropathology (TA, YS, HH, SF, SM) and Positron Medical Center (KI), Tokyo Metropolitan Institute of Gerontology; Departments of Pathology (HH, TA, MS), Radiology (AMT), and Neurology (KK), Tokyo Metropolitan General Hospital, Tokyo; Department of Molecular Genetics (AM, RK), Center for Bioresources, Brain Research Institute, Niigata University, Niigata; and Division of Neurology (TA, KN), Department of Brain and Neurosciences, Faculty of Medicine, Tottori University, Tottori, Japan.

Send correspondence and reprint requests to: Shigeo Murayama, MD, PhD, Department of Neuropathology, Tokyo Metropolitan Institute of Gerontology, 35-2 Sakaecho, Itabashi-ku, Tokyo 173-0015, Japan; E-mail: smurayam@tmig.or.jp

This study was supported by an Aid for Scientific Research on Priority Areas—Advanced Brain Science Project—from the Ministry of Education, Culture, Sports, Science, and Technology of Japan (S.M.).

A part of this study was presented at the 85th Annual Meeting of the American Association of Neuropathologists, June 2009, San Antonio, TX.

INTRODUCTION

Argyrophilic grains (AGs), first reported by Braak and Braak in 1987, consist of punctate or filiform structures in the neuropil that can be visualized by Gallyas-Braak silver staining (1). Dementia with grains (DG), as defined by Braak and Braak (1, 2) and Jellinger (3), is a form of senile dementia in which AGs are the sole morphological substrate that can explain the dementia. Argyrophilic grains accompanied neuronal cytoplasmic tau immunoreactivity (IR; pretangle), tau-positive astrocytes (bush-like astrocytes), oligodendroglial coiled bodies, and ballooned neurons (4). Ultrastructurally, AGs consist of a straight filament 9 to 18 nm in diameter and bundles of smooth tubules 25 nm in diameter and are thought to be localized in dendritic spines (5).

Argyrophilic grains consist of a 4-repeat isoform of tau protein (6–8), and antibodies directed against the 4-repeat tau are the most sensitive markers for the grains (9). We have reported that the severe involvement of the ambient gyrus is a unique pathological feature of DG (10, 11) and proposed a staging paradigm for AGs that starts with the involvement of the ambient gyrus and amygdala (Stage 1: ambient stage), then expands to include the posterior parahippocampal gyrus and medial anterior temporal pole (Stage 2: medial temporal stage), and finally spreads to the basal forebrain and anterior cingulate gyrus (Stage 3: frontal lobe stage) (12). Our staging scheme was recently supported by Ferrer et al (13) and Santpere and Ferrer (14).

In the process of screening unselected brains obtained from consecutive autopsy patients at our institute, we have frequently encountered asymmetry in the density or in the extent in AGs in cases that carry the abnormal structures. Because dementia in DG is usually associated with Stage 3 AG (12), we focused our investigation on this advanced stage of grain disease and characterized AG asymmetry in a systematic manner and correlated the findings with available neuroimaging. Our data on the asymmetry in the density and extent of grains, combined with the preferential atrophy of the ambient gyrus, may contribute to enhanced neuroimaging diagnosis of DG.

MATERIALS AND METHODS

Tissue Source

Brains and spinal cords were obtained from 653 consecutive autopsies at Tokyo Metropolitan Geriatric Hospital

Copyright © 2010 by the American Association of Neuropathologists, Inc. Unauthorized reproduction of this article is prohibited.

and Institute of Gerontology between June 2001 and December 2007. The ages of the subjects at death ranged from 52 to 104 years (mean ± SD = 81.1 ± 8.9 years), and the male-to-female ratio was 361:292.

Neuropathology

The brains and spinal cords were examined as previously reported (15). Briefly, one hemisphere was preserved for biochemical and molecular studies, and the other was prepared for morphological studies. At autopsy, 1 cerebral hemisphere was sliced in the coronal plane at 7-mm intervals. The brainstem was sectioned in the axial planes in 5-mm-thick slices, and the cerebellum was sectioned in sagittal planes in 5-mm-thick slices. The following anatomical areas were sampled: frontal, temporal, and occipital poles, parietal lobe including intraparietal sulcus, anterior amygdala, posterior hippocampus, dentate nucleus, and midbrain. The samples were fixed in 4% paraformaldehyde for 48 hours and embedded in paraffin. The other half of the brain was fixed in 20% buffered formalin for 7 to 13 days and sliced in the same manner as that performed in the contralateral hemisphere, and the representative areas were embedded in paraffin. We adjusted these fixation times for the frozen half and fixed half sides to compensate both for optimal fixation and for comparative morphological observations in AT8 immunohistochemistry (IHC) at the start of our brain bank in 1999. Six-micrometer-thick serial sections were stained with hematoxylin and eosin and by the Klüver-Barrera method. Selected sections were further examined with modified methenamine (16) and Gallyas-Braak (17) staining for senile changes, Congo red for amyloid deposition, and elastica Masson trichrome stain for vascular changes.

Immunohistochemistry

Selected sections were immunostained using an autostainer (Ventana 20NX; Ventana, Tucson, AZ), as previously reported (12). The antibodies included anti–phosphorylated tau (ptau; AT8, monoclonal; Innogenetics, Temse, Belgium), anti–4-repeat tau (RD4, monoclonal; Upstate, Lake Placid, NY), anti–phosphorylated α-synuclein (psyn; monoclonal, psyn no. 64 [18]), anti–β-amyloid 11–28 (12B2, monoclonal; IBL, Maebashi, Japan), antiubiquitin (polyclonal; DAKO, Glostrup, Denmark), and anti–phosphorylated TAR DNA-binding protein of 43 kd (TDP43; PSer409/410; monoclonal, a gift from Dr M. Hasegawa, Tokyo Institute of Psychiatry), as previously reported (18).

Apolipoprotein E Genotyping

Genomic DNA was extracted from freshly frozen kidneys of 577 patients (obtained from June 2001 to November 2006). DNA concentrations were measured with a spectrophotometer (U2000; Hitachi, Tokyo, Japan) adjusted to 100 μg/mL. Tissues from all but 7 patients (6 patients with Creutzfeldt-Jakob disease and 1 patient with global hypoxic ischemic changes) were genetically examined. After polymerase chain reaction amplification (19), apolipoprotein E (APOE) genotyping was conducted with the restriction enzyme *Hha*I, as described by Hixson and Vernier (20). From the freshly frozen brains of 69 patients (obtained from December 2006 to December 2007), APOE genotyping of all samples was performed by direct cycle sequencing with an ABI 3100 sequencer and a BigDye Terminator v3.1 kit (Applied Biosystems) using the following primers: C19APOE001-F (sense 5′-GCCTACAAATCGGAACTGGA-3′) and C19APOE001-R (antisense 5′- ACCTGCTCCTTCACCTCGT-3′) (21). AQ1

Clinical Data

Clinical information was retrospectively obtained from the medical charts as well as from interviews with patients' attending physicians and caregivers. The Mini-Mental State Examination (22) or Hasegawa Dementia Screening scale (or its revised version) (23) and the Instrumental Activities of Daily Living scale (24) were used to evaluate cognitive function. The Clinical Dementia Rating (CDR) scale (25) was retrospectively determined by 2 independent board-certified neurologists.

Neuropathological Diagnosis

Neurofibrillary tangles (NFTs) were classified into 7 stages (from 0 to 6), and senile plaques were classified into 4 stages (0 and from A to C) according to the criteria of Braak and Braak (26). Argyrophilic grains were classified into our 4 stages (from 0 to 3) as previously reported (12). The neuropathological diagnosis of Alzheimer disease (AD) was based on our definition (27), which proposes a modification of the National Institute on Aging–Reagan criteria. The diagnosis of DG and "neurofibrillary tangle–predominant form of senile dementia (NFTD)" was based on the definition of Jellinger (3) and Jellinger and Bancher (28). The diagnosis of dementia with Lewy bodies (DLB) was based on the revised consensus guidelines (29). The diagnosis of progressive supranuclear palsy (PSP) was based on the National Institute of Neurological Disorders and Stroke criteria (30). The diagnosis of corticobasal degeneration (CBD) was based on the National Institutes of Health criteria (31). The diagnosis of vascular dementia was based on the criteria of the National Institute of Neurological Disorders and Stroke Association Internationale pour la Recherche et l'Enseignement en Neurosciences (32).

Case Selection and Subclassification of Cases With AG Stage 3

All of the patients who were categorized into AG Stage 3 were subclassified into the following 4 forms: the "pure form" represented AGs without any vascular or neurodegenerative changes that could explain cognitive decline, fulfilling Braak NFT Stage 2 or lower and the brain bank for Aging Research Lewy Stage 1 or lower (33); the "NFT form" contained NFTs with the Braak NFT Stage 3 or higher and senile plaque Stage A or lower (26); the "mixed form" is complicated by vascular pathology or metabolic disorders that could explain the cognitive decline; and the "combined form" containing neurodegenerative pathology other than AG itself fulfilled the diagnostic criteria of certain demential disorders.

Evaluation of AGs and Related Structures

Argyrophilic grains were defined as round- or comma-shaped structures with a diameter greater than 1 μm in the neuropil. Bilateral sections of the anterior amygdala and posterior hippocampus at the level of the lateral geniculate body were stained with the Gallyas-Braak silver method and by IHC with AT8 and RD4. Gallyas-Braak silver staining was more sensitive for identifying AGs in 20% buffered

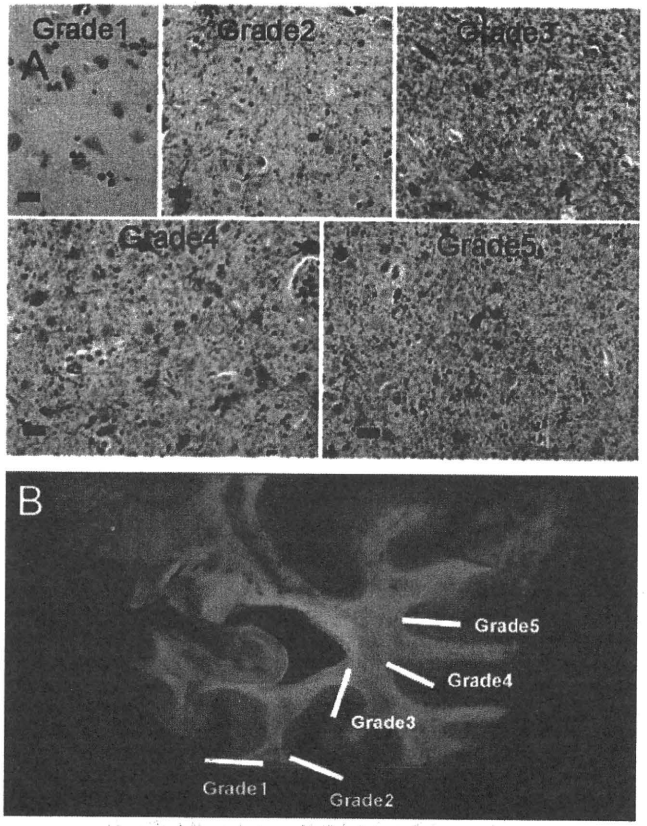

FIGURE 1. Extent and density grading of argyrophilic grains (AGs). **(A)** Density grades were obtained by counting AGs visualized with AT8 immunostain in high-power fields (HPFs; original magnification: 400×), in the entorhinal cortex at the level of the posterior hippocampus. Argyrophilic grains with a diameter greater than 1 μm were counted. Grade 1, 0 to 20/HPF; Grade 2, 20 to 50/HPF; Grade 3, 50 to 100/HPF; Grade 4, 100 to 200/HPF; Grade 5, greater than 200/HPF. Bar = 20 μm. **(B)** Argyrophilic grain extent grades were as follows: Grade 1, localized to the entorhinal cortex (parahippocampal gyrus); Grade 2, spreading to the crown of the fusiform gyrus (T4); Grade 3, to the valley of T4; Grade 4, to the inferior temporal gyrus; and Grade 5, to the middle temporal gyrus.

formalin-fixed sections than in 4% paraformaldehyde-fixed sections. In contrast, RD4 IHC was more sensitive for AGs in paraformaldehyde-fixed sections. AT8 IHC detected AGs to the same extent in both sections, as determined when we started our brain bank. Therefore, we compared the density of AG with AT8 IHC as follows: AGs were counted at a magnification of 400× in the basolateral nucleus of the bilateral amygdala and the entorhinal cortex of the posterior hippocampus and were classified to the following grades: Grade 1, 0 to 20; Grade 2, 20 to 50; Grade 3, 50 to 100; Grade 4, 100 to 200; and Grade 5, more than 200 (Fig. 1A).

To assess the extent of AGs, the following 5 grades were defined for AT8-stained sections of posterior hippocampus (Fig. 1B): Grade 1, localized to the entorhinal cortex (parahippocampal gyrus); Grade 2, spreading to the crown of fusiform gyrus (T4); Grade 3, to the valley of T4; Grade 4, to the inferior temporal gyrus (T3); and Grade 5, to the middle temporal gyrus (T2). Histopathological asymmetry was interpreted as present when there was any difference in the extent or density of grading between the 2 hemispheres.

We also counted the numbers of neuronal cytoplasmic AT8-IR inclusions (pretangles) in the granular layer of the dentate gyrus and classified them semiquantitatively as follows: Grade 1, 0 to 10/section; Grade 2, 10 to 40/section; Grade 3, 40 to 100/section; and Grade 4, more than 100/section. Asymmetry was defined when there was any difference between the right and left side.

Evaluation of Alzheimer-Type NFTs

In addition to Braak NFT stage, the AT8 staging of NFTs by the European Brain Net Consortium (34) was modified and used for this study. AT8 IHC was applied to the bilateral anterior amygdala, posterior hippocampi, and occipital cortex, and AT8 staging of the both sides was compared.

Evaluation of Clinical Images

Clinical images (computed tomography [CT], magnetic resonance imaging [MRI], *N*-isopropyl-^{123}I-*p*-iodoamphetamine single photon emission computed tomography [^{123}I-IMP-SPECT], ^{18}F-labeled fluorodeoxyglucose positron emission tomography [^{18}F-FDG-PET]) from our series were selected retrospectively and evaluated independently and blindly by 2 neurologists and a neuroradiologist (A.M.T.).

Statistical Analysis

Statistical analyses were performed with the χ^2 test or the Fisher exact test for comparisons of categorical data. Correlations between the extent and density grades of AGs in posterior hippocampus were assessed with the Spearman rank correlation coefficient. The Mann-Whitney *U* test was used for comparison of age at death, CDR score, and Braak NFT stage. All statistical analyses were performed using SPSS 15.0J for Windows (SPSS, Inc, Chicago, IL). The threshold for statistical significance was set at $p < 0.05$.

RESULTS

Clinical Data on Cognitive Decline

The CDR could be retrospectively assessed in 590 patients: CDR 0 (n = 214), CDR 0.5 (n = 85), CDR 1 (n = 123), CDR 2 (n = 40), and CDR 3 (n = 128). Thus, 63.7% had CDR 0.5 or higher (mild cognitive impairment or dementia).

TABLE 1. Correlation Between Extent and Density Grades of AGs in the Posterior Hippocampus

		Density Grade				
		1	2	3	4	5
Extent grade	1	10/6	0/1	0/0	0/0	0/0
	2	4/7	4/3	1/0	0/0	0/0
	3	4/2	3/1	3/3	2/2	0/0
	4	2/1	6/9	8/8	3/7	3/0
	5	1/0	0/3	3/5	6/5	2/2

The numbers correspond to right side/left side.
$r = 0.674$, $p < 0.001$.

TABLE 2. Demographic Data and Asymmetry in AGs in 65 Patients With AGs Stage 3

	Histopathological Asymmetry				Asymmetry in Each Grade			Dominant* Side		
	Total	No	Yes	p	Extent	Severity	p	Right	Left	p
No. cases	65	6	59		37	48		23	36	
Male/female	37:28	2:4	35:24	0.39	24:13	27:21	0.56	13:10	22:14	0.79
Age (years), mean ± SD	84.2 ± 7.6	88.5 ± 7.8	83.8 ± 7.4	0.15	83.1 ± 6.9	83.9 ± 7.4	0.57	84.1 ± 6.5	83.6 ± 7.9	0.81
CDR ≥ 0.5, n	56	5	51	0.13	30	46	0.83	19	32	0.94
CDR ≥ 1, n	42	4	38	0.07	22	35	0.66	15	23	0.60
APOE ε4 carriers	9	0	9	0.58	5	8	0.92	4	5	1.00
Braak NFT stage, mean	2.34	3.5	2.2	0.01	1.86	2.31	0.06	2.3	2.17	0.66
Braak SP stage, n										
0–A	44	4	40	0.58	27	32	0.69	17	23	0.51
B–C	21	2	19	0.57	10	16	0.70	6	13	0.32

*Side with greater either extent or density of AGs.
SP, senile plaque.

Neuropathological Diagnosis

The neuropathological diagnoses, excluding AG Stage 3 patients, consisted of AD (n = 71), Parkinson disease/Parkinson disease with dementia/DLB (n = 35), PSP (n = 14), vascular dementia (n = 12), NFTD (n = 12), amyotrophic lateral sclerosis (ALS)/ALS with dementia (n = 12), Creutzfeldt-Jakob disease (n = 6), hippocampal sclerosis (n = 6), CBD (n = 2), multiple-system atrophy (n = 3), Machado-Joseph disease (n = 3), Huntington disease (n = 2), and frontotemporal lobar degeneration with TDP43-IR inclusions (n = 1). Comorbid demential pathologies included AD plus DLB (n = 11), Parkinson disease with dementia plus PSP (n = 4), and AD plus vascular dementia (n = 1). The remaining patients did not fulfill clinical and/or pathological criteria for any single neurodegenerative disease.

Among the 653 subjects, 65 (10%) were classified into Brain Bank for Aging Research AG Stage 3. These 65 patients were further subclassified as pure form (n = 15, 23.1%), NFT form (n = 14, 21.5%), mixed form (n = 22, 33.8%), and combined form (n = 14, 21.5%). The degenerative pathological diagnoses of the combined form included PSP (n = 5), CBD (n = 3), AD (n = 2), DLB (n = 1), AD+DLB (n = 1), PSP + DLB (n = 1), ALS with dementia (n = 1), and ALS (n = 1).

Clinical Features of AG Stage 3 Patients

The ages at death of the 65 patients with AG Stage 3 ranged from 68 to 97 years (84.2 ± 7.6 years). The male-to-female ratio was 37:28. The CDR score could be retrospectively determined for 64 of these patients: CDR 0 (n = 8), CDR 0.5 (n = 14), CDR 1 (n = 17), CDR 2 (n = 5), and CDR 3 (n = 20). Thus, the CDR of 56 (87.5%) of the 64 patients was 0.5 or higher, corresponding to amnestic mild cognitive impairment or dementia. The clinical diagnoses of these patients were either AD or vascular dementia.

Histopathological Asymmetry of AGs and Related Structures

The histopathological asymmetry in the density grades of AG in the anterior amygdala was present in 32 (49.2%) of the 65 patients with AG Stage 3. The asymmetry was commensurate with the asymmetry in the density grades in the posterior hippocampus.

The extent and density grades of AG in the bilateral posterior hippocampus were strongly correlated (r = 0.674, $p < 0.001$; Table 1). Histopathological asymmetry was present in 59 (90.8%) of the 65 patients (Table 2). When compared in extent grade or in density grade alone, histopathological

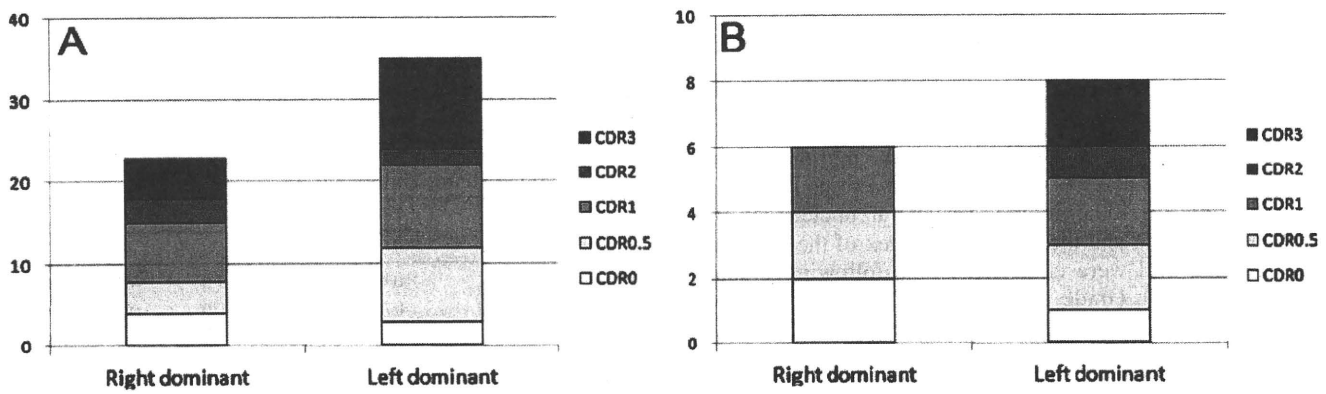

FIGURE 2. Clinical Dementia Rating scales. **(A)** Clinical Dementia Rating scores are not statistically significant among all subjects with argyrophilic grain Stage 3 (p = 0.735). **(B)** Of cases with the "pure form" of argyrophilic grain, only those with more extensive argyrophilic grain on the left side had Clinical Dementia Rating score of 2 or higher. The y axes indicate numbers of cases.

TABLE 3. Correlation of Pathological and Radiological Findings in Patients With AG Stage 3

		Histopathological Asymmetry			
		No	Yes		
	Total		Right-Dominant	Left-Dominant	*p
No. cases	65	6	23	36	
Morphological imaging	47 (CT, n = 39; MRI, n = 23)	5	17	25	
No asymmetry	27	5	6	16	
Right-dominant	11	0	11	0	
Left-dominant	9	0	0	9	<0.001
Functional imaging	7 (PET, n = 2; SPECT, n = 6)	0	3	4	
No asymmetry	0	0	0	0	
Right-dominant	3	0	3	0	
Left-dominant	4	0	0	4	<0.001

asymmetry was present in 37 (56.9%) or in 48 (73.8%) of the 65 patients, respectively. The mean age, male-to-female ratio, and mean Braak NFT stage of the 59 patients with asymmetry were 83.8 ± 7.4, 35:24, and 2.2, respectively; for the 6 patients without asymmetry, they were 88.5 ± 7.8, 2:4, and 3.5, respectively. Braak NFT stage was lower in patients with asymmetry than in patients with symmetry. Statistical difference was not shown between 2 sides when only the extent grade or the density grade was compared. There were 36 patients with left-sided predominance of AG and 23 with right-sided predominance. There was no difference in Braak NFT or senile plaque stage between the right-dominant and the left-dominant patients (Table 2). Although the difference of CDRs of all subjects with AG Stage 3 was not statistically significant, all patients classified as having the pure form and whose CDR was 2 or higher had left-sided predominance of AGs (Fig. 2). All 5 patients with AG Stage 3 combined with PSP and the 3 with CBD had histopathological asymmetry in AG that was commensurate with the histopathological asymmetry of PSP and CBD, i.e. histopathological asymmetry was evaluated in PSP patients semiquantitatively with respect to density of AT8-IR tangles and astrocytes in the bilateral sections of the dentate nucleus, red nucleus and frontal cortex, where the grain-related pretangles and bush-like astrocytes were rarely present. Asymmetry of pretangles in the granular cell layer of the dentate gyrus was present in 32 (49.2%) of 65 cases, which was commensurate with the asymmetry of AG.

Histologic and Neuroimaging Correlations

Computed tomographic and/or MRI scans were available in 47 patients for the evaluation of the asymmetry: CT alone (n = 24), MRI alone (n = 8), and both (n = 15). The mean interval between the last CT or MRI and death was 7 ± 15.6 months. There were 20 patients with asymmetry on CT and/or MRI, 9 with left side–dominant atrophy and 11 with right side–dominant atrophy. In each patient where asymmetry was detected, the direction of the asymmetry assessed by neuroimaging matched that of the histopathological asymmetry (Table 3). In the pure form, 6 (75%) of the 8 patients showed asymmetry in morphological imaging. On the other hand, 3 (37.5%) of the 8 patients in the NFT form, 8 (42.1%) of the 19 patients in the mixed form, and 3 (25%) of the 12 patients in the combined form showed asymmetry in morphological imaging, respectively. Among the 47 patients whose morphological imaging was available, 9 were examined more than twice; 8 of those patients (88.9%) had asymmetry in the first images (mean interval from imaging to death = 3 years 5 months ± 22 months) that was commensurate with the asymmetry in the last images. The remaining patient did not show asymmetry either in the first or in the last image. The sensitivity and specificity for detecting underlying histopathological asymmetry were 50% and 100% for CT and 59% and 100% for MRI. The histopathological differences in the density and extent scores were compared with the presence or absence of asymmetry in structural neuroimages; the more severe the histopathological asymmetry, the more often the asymmetry was present in the images (Table 4).

Functional neuroimages were available for the study of asymmetry in 7 patients, 6 of whom underwent ^{123}I-IMP-SPECT and 2 of whom underwent ^{18}F-FDG-PET. All the functional neuroimages showed asymmetry that correlated with histopathological asymmetry (Fig. 3).

Comparison of Asymmetry Between AG Stage 3 and AD

Among 56 of 71 patients with AD and AG lower than Stage 2 and without significant vascular pathology, histopathological asymmetry in NFT was present in 14 patients. Morphological imaging (CT in 39 patients and/or MRI in 21 patients) was available in 41 of the 56 patients (mean interval between the last CT or MRI and death was 10 ± 14.4 months);

TABLE 4. Correlation Between the Difference of Density or Extent Score and Morphological Asymmetry on Imaging in Patients With Histopathological Asymmetry

	Morphological Asymmetry	
	+	−
Score difference between hemispheres		
1	13	22
≥2	7	1

p = 0.01.
+, asymmetry present; −, no asymmetry.

8 (19.5%) of the 41 patients showed radiological asymmetry. Functional imaging (SPECT and/or PET) was available in 7 of 56 patients and in 4 of the 7 patients who had radiological asymmetry. The number of patients with AG Stage 3 and AD, with or without histopathological asymmetry, was 59 versus 6 in AG and 14 versus 42 in AD-type NFT ($p < 0.001$). Asymmetry in morphological imaging was more often present in AG Stage 3 (20/47, 42.6%) than in AD (12/44, 27.3%; $p < 0.05$).

Influence of APOE ε4 on AGs

The APOE genotypes of patients with AG Stage 3 were as follows: 1 patient with ε2/ε2, 3 patients with ε2/ε3, 52 patients with ε3/ε3, 9 patients with ε3/ε4, and none with

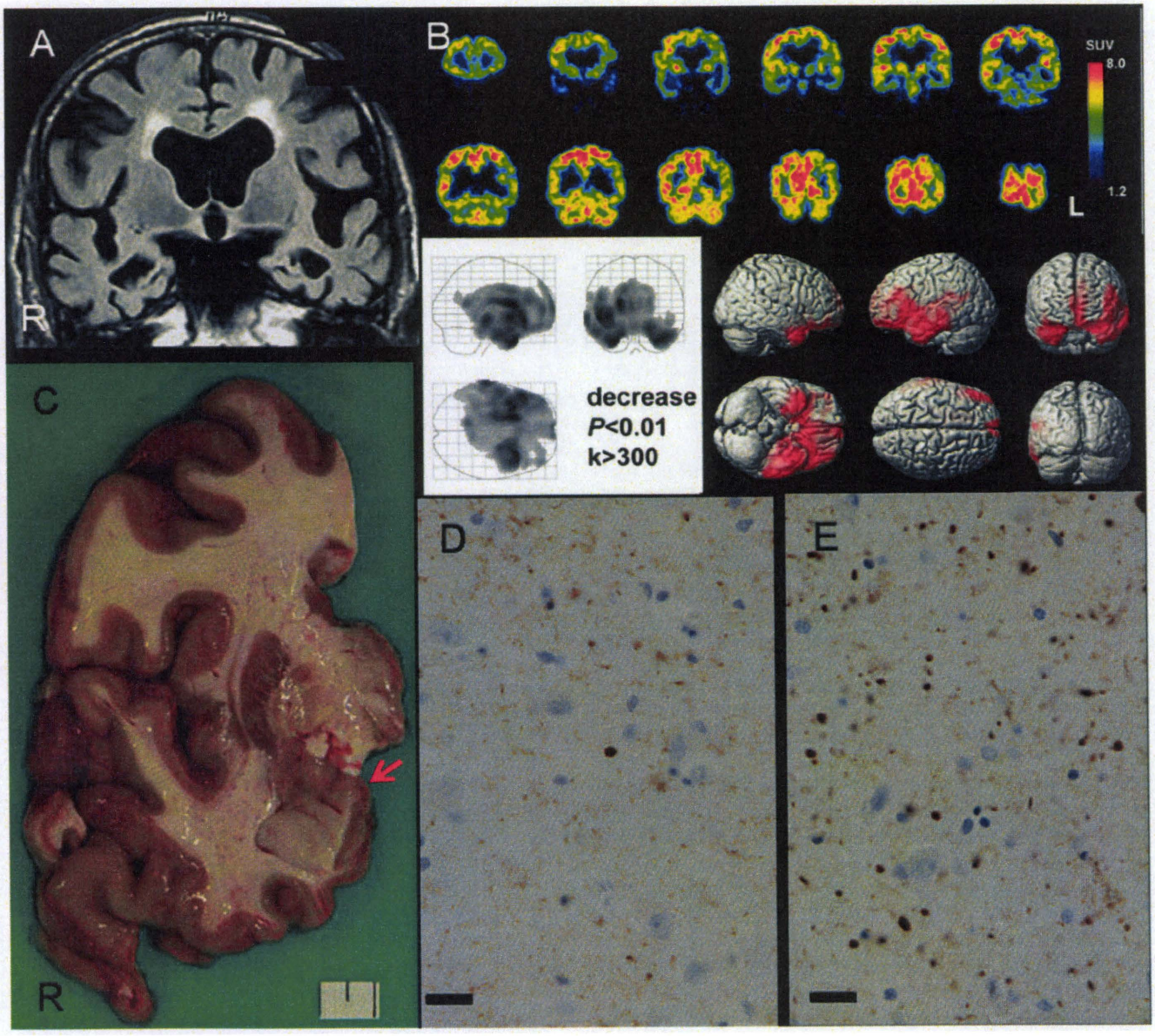

Fig 3 4/C

FIGURE 3. Images from an 86-year-old man diagnosed with pure form dementia with grains (Braak neurofibrillary tangle Stage 2, senile plaque Stage C [mainly diffuse plaques], or Clinical Dementia Rating 3). **(A)** In a cranial magnetic resonance image 4 years before death, there is dilatation of the temporal groove and inferior horn of the lateral ventricle and atrophy of the temporal pole and anterior medial temporal lobe, all with left side dominance. **(B)** A ^{18}F-labeled fluorodeoxyglucose positron emission tomographic image showing hypometabolism of the bilateral anterior medial temporal lobe with left side dominance. **(C)** Fresh coronal section of the right hemisphere showing marked atrophy of the amygdala and ambient gyrus (arrow). Scale = 1 cm. **(D, E)** At the level of the amygdala, there are many argyrophilic grains, with more on the left side **(E)** than on the right side **(D)**. AT8 immunostaining. Bar = 20 μm.

ε4/ε4. All 9 carriers of APOE ε4 showed histopathological asymmetry (statistically not significant vs noncarriers); of these, 1 patient had the pure form, 2 patients had the NFT form, 3 patients had the combined forms (1 patient each with PSP, DLB plus PSP, and CBD), and 3 patients had mixed forms.

DISCUSSION

We demonstrate histopathological asymmetry in the majority (59/65, 90.8%) of the brains examined from patients with AG Stage 3. Because this asymmetry can also be detected by neuroimaging in vivo, its identification may contribute to the clinical diagnosis of DG, particularly in combination with identification of preferential atrophy of the ambient gyrus, a hallmark of DG (10, 11).

The asymmetry in the posterior hippocampus was commensurate with the grain density of the anterior amygdala or the pretangles in the dentate gyrus. Asymmetry in grain density of the anterior amygdala was slightly less frequent than that of the posterior hippocampus, partly because the former seems to be involved in the initial stage of AG disease, and the density may be saturated at a later stage.

We also compared the bilateral maximum density of oligodendroglial coiled bodies in the white matter of parahippocampal gyrus, but there was extensive variability, and we could not perform statistical evaluation. The oligodendroglial coiled bodies observed in various neurodegenerative conditions may not be specific for AG disease.

The rate of detection of cases with histopathological asymmetry was 46.5% in structural neuroimages (CT or MRI) and 100% in functional neuroimages (^{123}I-IMP-SPECT/^{18}F-FDG-PET). The asymmetry in the structural neuroimages of the pure form alone reached 75%. Detection rates might increase if software were developed for voxel-based morphometry based on 3-dimensional MRI, focusing on asymmetry and selective atrophy of the ambient gyrus.

The frequent asymmetry in AG is shared with other tauopathies, including CBD, PSP, and Pick disease with Pick bodies. Patients with AG Stage 3 but without histopathological asymmetry were older and of higher Braak NFT stage than patients with asymmetry. This result may be partly influenced by the difficulty in discriminating AGs and Alzheimer-type neuropil threads in patients with higher Braak NFT stage, even with IHC using a specific antibody raised against the 4-repeat tau isoform (9). Alternatively, it may suggest a pathogenetic relationship between AGs and NFTs.

Argyrophilic grain Stage 3 cases showed asymmetry more often than AD cases by both histopathological and radiological assessments. Asymmetry may also be a feature of hippocampal sclerosis dementia (35), but these cases usually show asymmetry in signal intensity in the hippocampus in FLAIR images or do not show atrophy of the anterior medial temporal lobe, including amygdala (unpublished data).

Apolipoprotein E genotyping of subjects with AG Stage 3 did not demonstrate a correlation between asymmetry and ε2 (36–38). In contrast, although statistically not significant, all 9 ε4 carriers in the patients studied showed histopathological asymmetry. Apolipoprotein E ε4 consists of a risk factor of AD, and this may also be associated with the asymmetry of DG.

This analysis also indicates that patients with left-dominant AG tended to show more severe cognitive decline than patients with right-dominant AG. Among the 65 patients, 41 were right-handed, 1 was left-handed, and the rest did not have handedness recorded. Thus, the language center was most likely located in the left hemisphere in most cases, and it is reasonable to speculate that more extensive damage to the hemisphere dominant for language may result in more severe cognitive decline than involvement of the nondominant hemisphere. Retrospective studies of autopsy-confirmed DG reported that its clinical features are either AD-like amnesia (39–41) or Pick-like frontotemporal dementia (42–45). If clinical diagnosis of DG becomes possible and preferential involvement of either the right or the left hemisphere is determined radiologically, more detailed clinical and pathological correlations could be performed.

Few studies have examined the correlation between radiological and pathological findings of DG. In a postmortem MRI study of the oldest patients (>85 years) with special attention to atrophy of the medial temporal lobe, Barkhof et al (46) reported that 13 (10%) of 132 patients had pure AG disease; 4 of the 13 patients showed significant atrophy involving the medial temporal lobe. Josephs et al (47) used voxel-based morphometry to analyze MRI of AG patients with or without dementia and concluded that the damage visible in the MR image contributed to the clinical manifestation of dementia; however, they did not mention either radiological or pathological asymmetry.

Argyrophilic grains are often associated with other neurodegenerative processes. Because NFT-dominant senile changes are frequently associated with AGs and could modify clinical manifestations, we separated the NFT form from other cases for future analysis. It is notable that all PSP patients with AG Stage 3 showed the commensurate histopathological asymmetry, suggesting that histopathological asymmetry of PSP may be influenced by the histopathological asymmetry of AGs.

In conclusion, left-right asymmetry in density and/or extent of AG is present in most patients with AG Stage 3 and is detectable by antemortem morphological and functional neuroimaging. In combination with the finding of preferential atrophy of the ambient gyrus, detection of this asymmetry could contribute to the clinical diagnosis of DG.

ACKNOWLEDGMENTS

The authors thank Mr Naoo Aikyo, Mr Fumio Hasegawa, Ms Mieko Harada, Ms Yuki Kimura, and Ms Nobuko Naoi for the preparation of sections and Dr Kinuko Suzuki for helpful discussions. The authors also thank 2 anonymous neurologists for preparing the CDR ratings used in this study.

REFERENCES

1. Braak H, Braak E. Argyrophilic grains: Characteristic pathology of cerebral cortex in cases of adult onset dementia without Alzheimer changes. Neurosci Lett 1987;76:124–27

2. Braak H, Braak E. Argyrophilic grain disease: Frequency of occurrence in different age categories and neuropathological diagnostic criteria. J Neural Transm 1998;105:801–19
3. Jellinger KA. Dementia with grains (argyrophilic grain disease). Brain Pathol 1998;8:377–86
4. Tolnay M, Clavaguera F. Argyrophilic grain disease: A late-onset dementia with distinctive features among tauopathies. Neuropathology 2004;24:269–83
5. Ikeda K, Akiyama H, Kondo H, et al. A study of dementia with argyrophilic grains. Possible cytoskeletal abnormality in dendrospinal portion of neurons and oligodendroglia. Acta Neuropathol 1995;89:409–14
6. Togo T, Sahara N, Yen SH, et al. Argyrophilic grain disease is a sporadic 4-repeat tauopathy. J Neuropathol Exp Neurol 2002;61:547–56
7. Tolnay M, Sergeant N, Ghestem A, et al. Argyrophilic grain disease and Alzheimer's disease are distinguished by their different distribution of tau protein isoforms. Acta Neuropathol 2002;104:425–34
8. Zhukareva V, Shah K, Uryu K, et al. Biochemical analysis of tau proteins in argyrophilic grain disease, Alzheimer's disease, and Pick's disease: A comparative study. Am J Pathol 2002;161:1135–41
9. Fujino Y, Wang DS, Thomas N, et al. Increased frequency of argyrophilic grain disease in Alzheimer disease with 4*R* tau-specific immunohistochemistry. J Neuropathol Exp Neurol 2005;64:209–14
10. Saito Y, Yamazaki M, Kanazawa I, et al. Severe involvement of the ambient gyrus in a case of dementia with argyrophilic grain disease. J Neurol Sci 2002;196:71–75
11. Saito Y, Nakahara K, Yamanouchi H, et al. Severe involvement of ambient gyrus in dementia with grains. J Neuropathol Exp Neurol 2002; 61:789–96
12. Saito Y, Ruberu NN, Sawabe M, et al. Staging of argyrophilic grains: An age-associated tauopathy. J Neuropathol Exp Neurol 2004;63:911–18
13. Ferrer I, Santpere G, van Leeuwen FW. Argyrophilic grain disease. Brain 2008;131:1416–32
14. Santpere G, Ferrer I. Delineation of early changes in cases with progressive supranuclear palsy-like pathology. Astrocytes in striatum are primary targets of tau phosphorylation and GFAP oxidation. Brain Pathol 2009;19:177–87
15. Fumimura Y, Ikemura M, Saito Y, et al. Analysis of the adrenal gland is useful for evaluating pathology of the peripheral autonomic nervous system in Lewy body disease. J Neuropathol Exp Neurol 2007;66: 354–62
16. Yamaguchi H, Haga C, Hirai S, et al. Distinctive, rapid, and easy labeling of diffuse plaques in the Alzheimer brains by a new methenamine silver stain. Acta Neuropathol 1990;79:569–72
17. Gallyas F. Silver staining of Alzheimer's neurofibrillary changes by means of physical development. Acta Morphol Acad Sci Hung 1971; 19:1–8
18. Saito Y, Kawashima A, Ruberu NN, et al. Accumulation of phosphorylated alpha-synuclein in aging human brain. J Neuropathol Exp Neurol 2003;62:644–54
19. Wenham PR, Price WH, Blandell G. Apolipoprotein E genotyping by one-stage PCR. Lancet 1991;337:1158–59
20. Hixson JE, Vernier DT. Restriction isotyping of human apolipoprotein E by gene amplification and cleavage with *Hha*I. J Lipid Res 1990;31: 545–48
21. Kuwano R, Miyashita A, Arai H, et al. Dynamin-binding protein gene on chromosome 10q is associated with late-onset Alzheimer's disease. Hum Mol Genet 2006;15:2170–82
22. Folstein MF, Folstein SE, McHugh PR. "Mini-Mental State." A practical method for grading the cognitive state of patients for the clinician. J Psychiatr Res 1975;12:189–98
AQ2 23. Hasegawa KI IK, Moriya K. An investigation of dementia rating scale for the elderly. Seishin Igaku 1974;16:965–69
24. Lawton MP, Brody EM. Assessment of older people: Self-maintaining and instrumental activities of daily living. Gerontologist 1969;9:179–86
25. Hughes CP, Berg L, Danziger WL, et al. A new clinical scale for the staging of dementia. Br J Psychiatry 1982;140:566–72
26. Braak H, Braak E. Neuropathological stageing of Alzheimer-related changes. Acta Neuropathol 1991;82:239–59
27. Murayama S, Saito Y. Neuropathological diagnostic criteria for Alzheimer's disease. Neuropathology 2004;24:254–60
28. Jellinger KA, Bancher C. Senile dementia with tangles (tangle predominant form of senile dementia). Brain Pathol 1998;8:367–76
29. McKeith IG, Dickson DW, Lowe J, et al. Diagnosis and management of dementia with Lewy bodies: Third report of the DLB Consortium. Neurology 2005;65:1863–72
30. Hauw JJ, Daniel SE, Dickson D, et al. Preliminary NINDS neuropathologic criteria for Steele-Richardson-Olszewski syndrome (progressive supranuclear palsy). Neurology 1994;44:2015–19
31. Dickson DW, Bergeron C, Chin SS, et al. Office of Rare Diseases neuropathologic criteria for corticobasal degeneration. J Neuropathol Exp Neurol 2002;61:935–46
32. Roman GC, Tatemichi TK, Erkinjuntti T, et al. Vascular dementia: Diagnostic criteria for research studies. Report of the NINDS-AIREN International Workshop. Neurology 1993;43:250–60
33. Saito Y, Ruberu NN, Sawabe M, et al. Lewy body–related alpha-synucleinopathy in aging. J Neuropathol Exp Neurol 2004;63:742–49
34. Alafuzoff I, Arzberger T, Al-Sarraj S, et al. Staging of neurofibrillary pathology in Alzheimer's disease: A study of the BrainNet Europe Consortium. Brain Pathol 2008;18:484–96
35. Probst A, Taylor KI, Tolnay M. Hippocampal sclerosis dementia: A reappraisal. Acta Neuropathol 2007;114:335–45
36. Ghebremedhin E, Schultz C, Botez G, et al. Argyrophilic grain disease is associated with apolipoprotein E epsilon 2 allele. Acta Neuropathol 1998; 96:222–24
37. Togo T, Cookson N, Dickson DW. Argyrophilic grain disease: Neuropathology, frequency in a dementia brain bank and lack of relationship with apolipoprotein E. Brain Pathol 2002;12:45–52
38. Tolnay M, Probst A, Monsch AU, et al. Apolipoprotein E allele frequencies in argyrophilic grain disease. Acta Neuropathol 1998;96: 225–27
39. Saito Y, Murayama S. Neuropathology of mild cognitive impairment. Neuropathology 2007;27:578–84
40. Petersen RC, Parisi JE, Dickson DW, et al. Neuropathologic features of amnestic mild cognitive impairment. Arch Neurol 2006;63:665–72
41. Jicha GA, Petersen RC, Knopman DS, et al. Argyrophilic grain disease in demented subjects presenting initially with amnestic mild cognitive impairment. J Neuropathol Exp Neurol 2006;65:602–9
42. Steuerwald GM, Baumann TP, Taylor KI, et al. Clinical characteristics of dementia associated with argyrophilic grain disease. Dement Geriatr Cogn Disord 2007;24:229–34
43. Togo T, Isojima D, Akatsu H, et al. Clinical features of argyrophilic grain disease: A retrospective survey of cases with neuropsychiatric symptoms. Am J Geriatr Psychiatry 2005;13:1083–91
44. Ikeda K, Akiyama H, Arai T, et al. Clinical aspects of argyrophilic grain disease. Clin Neuropathol 2000;19:278–84
45. Ishihara K, Araki S, Ihori N, et al. Argyrophilic grain disease presenting with frontotemporal dementia: A neuropsychological and pathological study of an autopsied case with presenile onset. Neuropathology 2005;25: 165–70
46. Barkhof F, Polvikoski TM, van Straaten EC, et al. The significance of medial temporal lobe atrophy: A postmortem MRI study in the very old. Neurology 2007;69:1521–27
47. Josephs KA, Whitwell JL, Parisi JE, et al. Argyrophilic grains: A distinct disease or an additive pathology? Neurobiol Aging 2008;29:566–73

doi:10.1093/brain/awq216 Brain 2010: 133; 3043–3057 | 3043

BRAIN
A JOURNAL OF NEUROLOGY

Prospective 10-year surveillance of human prion diseases in Japan

Ichiro Nozaki,[1,2] Tsuyoshi Hamaguchi,[1] Nobuo Sanjo,[3,4] Moeko Noguchi-Shinohara,[1] Kenji Sakai,[1] Yosikazu Nakamura,[4,5] Takeshi Sato,[4,6] Tetsuyuki Kitamoto,[4,7] Hidehiro Mizusawa,[3,4] Fumio Moriwaka,[4,8] Yusei Shiga,[4,9] Yoshiyuki Kuroiwa,[4,10] Masatoyo Nishizawa,[4,11] Shigeki Kuzuhara,[4,12] Takashi Inuzuka,[4,13] Masatoshi Takeda,[4,14] Shigetoshi Kuroda,[4,15] Koji Abe,[4,16] Hiroyuki Murai,[4,17] Shigeo Murayama,[4,18] Jun Tateishi,[4,19] Ichiro Takumi,[4,20] Susumu Shirabe,[4,21] Masafumi Harada,[4,22] Atsuko Sadakane[5] and Masahito Yamada[1,4]

1 Department of Neurology and Neurobiology of Aging, Kanazawa University Graduate School of Medical Science, Kanazawa, Japan
2 Department of Neurology, Noto General Hospital, Nanao, Japan
3 Department of Neurology and Neurological Science, Graduate School, Tokyo Medical and Dental University, Tokyo, Japan
4 Creutzfeldt–Jakob Disease Surveillance Committee, Japan
5 Department of Public Health, Jichi Medical University, Shimotsuke, Japan
6 Department of Neurology, Higashi Yamato Hospital, Higashiyamato, Japan
7 Department of Prion Protein Research, Division of CJD Science and Technology, Tohoku University Graduate School of Medicine, Sendai, Japan
8 Department of Communication Disorders, Health Sciences University of Hokkaido Graduate School of Psychological Science, Ishikari, Japan
9 Department of Neurology, Aoba Neurosurgical Clinic, Sendai, Japan
10 Department of Neurology, Yokohama City University School of Medicine, Yokohama, Japan
11 Department of Neurology, Brain Research Institute, Niigata University, Niigata, Japan
12 Department of Neurology, National Center Hospital of Neurology and Psychiatry, Tokyo, Japan
13 Department of Neurology and Geriatrics, Gifu University Graduate School of Medicine, Gifu, Japan
14 Department of Psychiatry, Osaka University Graduate School of Medicine, Suita, Japan
15 Department of Neuropsychiatry, Graduate School of Medicine, Dentistry and Pharmaceutical Sciences, Okayama University, Okayama, Japan
16 Department of Neurology, Graduate School of Medicine, Dentistry and Pharmaceutical Science, Okayama University, Okayama, Japan
17 Department of Neurology, Iizuka Hospital, Fukuoka, Japan
18 Department of Neuropathology, Tokyo Metropolitan Institute of Gerontology, Tokyo, Japan
19 Harukaze Healthcare Service Institution, Fukuoka, Japan
20 Department of Neurosurgery, Nippon Medical School Musashi Kosugi Hospital, Kawasaki, Japan
21 Centre of Health and Community Medicine, Nagasaki University, Nagasaki, Japan
22 Department of Medical Imaging, Institute of Health Biosciences, the University of Tokushima Graduate School, Tokushima, Japan

Correspondence to: Masahito Yamada,
Department of Neurology and Neurobiology of Ageing,
Kanazawa University Graduate School of Medical Science,
13-1 Takara-machi,
Kanazawa 920-8640, Japan
E-mail: m-yamada@med.kanazawa-u.ac.jp

We analysed the epidemiological data and clinical features of patients with prion diseases that had been registered by the Creutzfeldt-Jakob Disease Surveillance Committee, Japan, over the past 10 years, since 1999. We obtained information on 1685 Japanese patients suspected as having prion diseases and judged that 1222 patients had prion diseases, consisting of definite ($n = 180$, 14.7%) and probable ($n = 1029$, 84.2%) cases, except for dura mater graft-associated Creutzfeldt–Jakob disease which also included possible cases ($n = 13$, 1.1%). They were classified into 922 (75.5%) with sporadic Creutzfeldt–Jakob disease, 216

Received May 1, 2010. Revised June 14, 2010. Accepted June 15, 2010. Advance Access publication September 20, 2010
© The Author (2010). Published by Oxford University Press on behalf of the Guarantors of Brain. All rights reserved.
For Permissions, please email: journals.permissions@oxfordjournals.org

Downloaded from brain.oxfordjournals.org at Tokyo Metropolitan Institute of Gerontology on January 25, 2011

(17.7%) with genetic prion diseases, 81 (6.6%) with acquired prion diseases, including 80 cases of dura mater graft-associated Creutzfeldt–Jakob disease and one case of variant Creutzfeldt–Jakob disease, and three cases of unclassified Creutzfeldt–Jakob disease (0.2%). The annual incidence rate of prion disease ranged from 0.65 in 1999 to 1.10 in 2006, with an average of 0.85, similar to European countries. Although methionine homozygosity at codon 129 polymorphism of the prion protein gene was reported to be very common (93%) in the general Japanese population, sporadic Creutzfeldt–Jakob disease in Japan was significantly associated with codon 129 homozygosity (97.5%), as reported in western countries. In sporadic Creutzfeldt–Jakob disease, MM1 type (Parchi's classification) is the most common, as in western countries. Among atypical sporadic Creutzfeldt–Jakob disease cases, the MM2 type appeared most common, probably related to the very high proportion of methionine allele in the Japanese population. As for iatrogenic Creutzfeldt–Jakob disease, only dura mater graft-associated Creutzfeldt–Jakob disease cases were reported in Japan and, combined with the data from previous surveillance systems, the total number of dura mater graft-associated Creutzfeldt–Jakob disease was 138, comprising the majority of worldwide dura mater graft-associated Creutzfeldt–Jakob disease patients. Regarding genetic prion diseases, the most common mutation of prion protein gene was V180I (41.2%), followed by P102L (18.1%), E200K (17.1%) and M232R (15.3%), and this distribution was quite different from that in Europe. In particular, V180I and M232R were quite rare mutations worldwide. Patients with V180I or M232R mutations rarely had a family history of prion diseases, indicating that a genetic test for sporadic cases is necessary to distinguish these from sporadic Creutzfeldt–Jakob disease. In conclusion, our prospective 10-year surveillance revealed a frequent occurrence of dura mater graft-associated Creutzfeldt–Jakob disease, and unique phenotypes of sporadic Creutzfeldt–Jakob disease and genetic prion diseases related to the characteristic distribution of prion protein gene mutations and polymorphisms in Japan, compared with those in western countries.

Keywords: prion disease; dura mater graft-associated Creutzfeldt–Jakob disease; 14-3-3 protein; periodic synchronous wave complexes; codon 129 or 219 polymorphism

Abbreviations: PrP = prion protein; PSWC = periodic synchronous wave complex; WHO = World Health Organization

Introduction

Prion diseases are a fatal human transmissible spongiform encephalopathy (Prusiner, 1998) and are classified into sporadic, genetic and acquired forms; the most common being sporadic Creutzfeldt–Jakob disease, which is of unknown aetiology. The overall annual mortality rate of sporadic Creutzfeldt–Jakob disease is ~1.5 per million worldwide (Ladogana *et al.*, 2005). The genetic form (i.e. genetic prion disease) is defined as a prion disease with causative mutations in the human prion protein (PrP) gene (*PrP*) and/or a relevant family history, including Gerstmann–Sträussler–Scheinker disease, fatal familial insomnia and genetic Creutzfeldt–Jakob disease (Kovács *et al.*, 2005). The acquired forms are transmitted among humans (i.e. iatrogenic Creutzfeldt–Jakob disease or Kuru) or from animals to humans, particularly bovine to human (i.e. variant Creutzfeldt–Jakob disease). To date, >400 patients with iatrogenic Creutzfeldt–Jakob disease have been reported, including transmission via infectious PrP-contaminated neurosurgical instruments, deep brain electrodes, human pituitary growth hormone, human cadaveric dura mater grafts, corneal transplantation or blood transfusion (Brown *et al.*, 2006). In particular, >50% of patients with cadaveric dura mater graft-associated Creutzfeldt–Jakob disease have occurred in Japan (Brown *et al.*, 2006). Although our previous case-control study revealed that medical procedures before the onset of prion diseases did not influence the onset of sporadic Creutzfeldt–Jakob disease, there was a problem that surgical treatments were performed on some patients with sporadic Creutzfeldt–Jakob disease after the onset of prion diseases (Hamaguchi *et al.*, 2009*a*, *b*). Since the first identification of variant Creutzfeldt–Jakob disease in the UK in 1996, 212 patients have been reported worldwide, including in Canada, France, Ireland, Italy, Japan, Portugal, Saudi Arabia, Spain, the Netherlands and the USA as well as the UK [The National Creutzfeldt–Jakob Disease Surveillance Unit (NCJDSU) (http://www.cjd.ed.ac.uk/vcjdworld.htm)].

From the viewpoint of public health, identification of the incidence of human and animal prion diseases is essential to prevent disease transmission. Various Creutzfeldt–Jakob disease surveillance systems have been established since the 1990s in many countries, including Australia, Austria, Belgium, Canada, Catalonia, China, France, Germany, Ireland, Italy, Slovakia, Spain, Switzerland, the Netherlands, the UK, the USA and Japan (Will *et al.*, 1998; Nakamura *et al.*, 1999; Collins *et al.*, 2002; Glatzel *et al.*, 2002; Puopolo *et al.*, 2003; Horan *et al.*, 2004; Pocchiari *et al.*, 2004; Sanchez-Valle *et al.*, 2004; Ladogana *et al.*, 2005; de Pedro-Cuesta *et al.*, 2006; Van Everbroeck *et al.*, 2006; Heinemann *et al.*, 2007; Shi *et al.*, 2008; Klug *et al.*, 2009; Holman *et al.*, 2010).

Although detailed data from the nationwide surveillance of human prion diseases have been published by European countries, Australia and the USA (Ladogana *et al.*, 2005; de Pedro-Cuesta *et al.*, 2006; Heinemann *et al.*, 2007; Klug *et al.*, 2009; Holman *et al.*, 2010), large-scale prospective data, comparable to those from western countries, have never been reported from Asia. In Japan, the current Creutzfeldt–Jakob disease surveillance system was established in 1999 (Noguchi-Shinohara *et al.*, 2007) and prospective nationwide surveillance has been ongoing for

>10 years. Here we report the prospective 10-year data of the Japanese Creutzfeldt–Jakob disease surveillance.

Materials and methods

Patients and ethical aspects

In Japan, the prospective surveillance of human prion disease by the Creutzfeldt–Jakob Disease Surveillance Committee started in April 1999. Japan was divided into 10 areas for surveillance. The Creutzfeldt–Jakob Disease Surveillance Committee, with 19 members, included members responsible for surveillance in each area, and for epidemiology, neuroimaging, genetic analysis, CSF tests, western blotting and neuropathology. Information on patients with suspected prion diseases was obtained through (i) the registration of each patient's family with the Intractable Disease Treatment Research Program, the Ministry of Health, Labour and Welfare, Japan; (ii) notification based on the Infectious Diseases Control Law; or (iii) a request for genetic or CSF analyses by physicians to the members of the Creutzfeldt–Jakob disease Surveillance Committee. Written informed consent to participate in the study was given by all patients' families. The study protocol was approved by the Medical Ethics Committee of Kanazawa University. We analysed all patients suspected of prion disease who had been registered by the Creutzfeldt–Jakob Disease Surveillance Committee in Japan from April 1999 to September 2009. Each patient suspected of having prion disease was investigated by the members of the Creutzfeldt–Jakob Disease Surveillance Committee in cooperation with Creutzfeldt–Jakob disease specialist(s) in each prefecture using the following surveillance protocol: previous medical history, clinical history, neurological findings, laboratory data including analyses of biomarkers (i.e. 14-3-3 protein) in CSF, MRI or CT, analyses of cerebral blood flow by single photon emission computed tomography, EEG, genetic analyses of *PrP*, neuropathological examinations and western blot analyses of protease K-resistant PrP. Based on discussions with the Creutzfeldt–Jakob Disease Surveillance Committee using the case definition shown below, we decided whether they had prion diseases.

Case definition

Prion diseases were classified into four categories: (i) sporadic Creutzfeldt–Jakob disease, (ii) acquired prion diseases (iatrogenic Creutzfeldt–Jakob disease or variant Creutzfeldt–Jakob disease), (iii) genetic prion diseases and (iv) unclassified prion diseases. Sporadic Creutzfeldt–Jakob disease was diagnosed according to the classical criteria established by Masters *et al.* (1979). The World Health Organization (WHO) criteria (WHO, 1998) were not applied because the assay of CSF 14-3-3 protein, which is required by the WHO criteria, was not standardized in Japan until April 2009. Regarding acquired prion diseases, iatrogenic Creutzfeldt–Jakob disease was diagnosed using the criteria for sporadic Creutzfeldt–Jakob disease. Cases of dura mater graft-associated Creutzfeldt–Jakob disease are categorized into two subtypes: the plaque type, which shows plaque-type PrP deposits, and the non-plaque type, which shows synaptic-type PrP deposits without PrP plaques (Noguchi-Shinohara *et al.*, 2007; Yamada *et al.*, 2009). Variant Creutzfeldt–Jakob disease was diagnosed using the WHO (2001) criteria. Genetic prion disease was diagnosed by neuropsychiatric findings compatible with prion disease, a relevant family history and a mutation of *PrP*. In patients with the M232R mutation, Shiga *et al.* (2007) reported two different clinical types: a rapidly progressive type that developed to akinetic mutism within 6 months (rapid type) and a slowly progressive type that did not develop to akinetic mutism until 15 months (slow type) (Shiga *et al.*, 2007). Unclassified Creutzfeldt–Jakob disease was defined as cases requiring more information (e.g. history of protease K-resistant PrP-contaminated medical procedure) for classification.

The accuracy of the diagnosis of prion disease was defined as: (i) 'definite', i.e. pathologically verified cases; (ii) 'probable', i.e. cases with neuropsychiatric manifestations compatible with prion diseases and periodic synchronous wave complexes (PSWCs) on EEG without pathological examinations, or cases of genetic prion disease with mutations of *PrP*; (iii) 'possible', i.e. cases with the same findings as 'probable' Creutzfeldt–Jakob disease, but no PSWCs on EEG or genetic prion disease cases with relevant family histories but without analyses of *PrP*.

The instances that did not satisfy the case definition of prion diseases were classified into three categories: (i) 'prion diseases definitely denied', (ii) 'prion diseases probably denied', and (iii) 'diagnosis unclear'. 'Prion diseases definitely denied' included patients who could be given a definite diagnosis of other diseases, and 'prion diseases probably denied' included patients in whom prion diseases were denied due to an improving, stable disease course or other reasons without a definite diagnosis of other diseases. 'Diagnosis unclear' was defined as such.

Clinical analyses and laboratory examinations

We analysed the age at onset of prion disease, sex, clinical duration between onset and akinetic mutism or death (if patients did not develop akinetic mutism), neuropsychiatric symptoms and signs during the clinical course, duration between the onset and appearance of each neuropsychiatric finding, brain MRI findings, PSWCs on EEG, *PrP* genotypes and CSF 14-3-3 protein. In iatrogenic Creutzfeldt–Jakob disease cases, the following points were investigated: year and age of receiving the medical procedure contaminated with prions, incubation period between receiving the transplanted graft and onset of Creutzfeldt–Jakob disease, source of the medical procedure and the type of surgery. PSWCs on EEG were judged to be 'typical' or 'suggested' by member(s) of the Creutzfeldt–Jakob Disease Surveillance Committee responsible for each area. The 'typical' cases were reported to be 'positive'. For the 'suggested' cases, the findings of the EEG were reviewed and discussed by the committee to decide 'positive' or 'negative' for PSWCs. High intensities on the following MRI sequences were examined in the cerebral cortices, basal ganglia and thalamus: diffusion-weighted images, fluid-attenuated inversion recovery images, or T_2-weighted images. The hyperintensities on MRI were defined as high signals in the basal ganglia and/or cerebral cortices, either in T_2-weighted images, fluid-attenuated inversion recovery images or diffusion-weighted images, which were compatible with the radiological findings of prion diseases except for variant Creutzfeldt–Jakob disease; hyperintensity on MRI in variant Creutzfeldt–Jakob disease was defined according to the WHO diagnostic criteria (WHO 2001). As reported earlier, the CSF 14-3-3 protein immunoassay was examined by western blotting of CSF with the polyclonal antibody for the β isoform (Santa Cruz Biotechnology, Santa Cruz, CA, USA) or the polyclonal antibody for the γ isoform (Takahashi *et al.*, 1999; Satoh *et al.*, 2006). *PrP* was analysed in the open reading frame after extracting DNA from patients' blood, as described earlier (Kitamoto *et al.*, 1992, 1993).

Neuropathological examinations and western blot analyses of protease K-resistant PrP

Brain sections were stained with routine techniques; immunohistochemistry was performed with mouse monoclonal antibody 3F4 (Senetek, MD Heights, MO, USA) (Kitamoto *et al.*, 1992). Frozen brain tissues were homogenized and western blot analyses of protease K-resistant PrP were performed with 3F4 as described earlier (Shimizu *et al.*, 1999).

Statistical analysis

Differences were assessed among three types of prion diseases (sporadic Creutzfeldt–Jakob disease, dura mater graft-associated Creutzfeldt–Jakob disease and genetic prion diseases), between subtypes of sporadic Creutzfeldt–Jakob disease according to Parchi's classification (Parchi *et al.*, 1999) and between *PrP* mutation groups of genetic prion disease with respect to age at onset or clinical duration by using one-factor ANOVA, and by positive findings of laboratory studies using the chi-square test or Fisher's exact probability test. Statistical significance was defined as $P<0.05$. Statistical analyses were performed using StatView® J-7.5 (Abacus Concepts, Berkeley, CA, USA). Crude, age- and sex-specific incidence rates were calculated using denominator population data for 2005 provided by the Statistics Bureau, the Ministry of Internal Affairs and Communications, Japan (http://www.stat.go.jp/english/data/kokusei/2005/poj/mokuji.htm). Age-adjusted incidence rate by sex was calculated by the direct method using population data for 2005. Data on the number of deaths from prion diseases were obtained by Vital Statistics of Japan (Statistics and Information Department, Ministers Secretariat, Ministry of Health, Labour and Welfare, 2009) and the mortality rate was calculated using denominator population data for 2005.

Results

Overall characteristics and classification of prion disease

The Creutzfeldt–Jakob Disease Surveillance Committee obtained information on 1685 patients suspected as having prion disease during the 10 years between April 1999 and September 2009. After the surveillance, 1324 patients were judged to have prion diseases, including definite ($n=180$, 13.6%), probable ($n=1029$, 77.7%) or possible ($n=115$, 8.7%) cases. There were 264 patients with 'prion disease definitely denied' or 'prion disease probably denied' (Table 1) and 61 patients with 'diagnosis unclear'.

We analysed the characteristics and laboratory data of only definite and probable cases, except for dura mater graft-associated Creutzfeldt–Jakob disease. As patients with plaque-type dura mater graft-associated Creutzfeldt–Jakob disease show mostly progressive ataxia without PSWCs and do not satisfy the criteria of 'probable' (Noguchi-Shinohara *et al.*, 2007; Yamada *et al.*, 2009), possible cases were included in the analysis.

Consequently, 1222 patients were analysed and classified into 922 (75.5%) with sporadic Creutzfeldt–Jakob disease, 216 (17.7%) with genetic prion diseases, 81 (6.6%) with acquired prion diseases, including 80 cases of dura mater graft-associated Creutzfeldt–Jakob disease and 1 case of variant Creutzfeldt–Jakob disease, and 3 cases of unclassified Creutzfeldt–Jakob disease (0.2%) (Table 2). There were no iatrogenic Creutzfeldt–Jakob disease cases other than dura mater graft-associated Creutzfeldt–Jakob disease.

Table 1 Diagnoses in 264 patients with prion disease definitely or probably denied

Diagnosis	Number of cases
Encephalitis[a]	32
Alzheimer's disease	28
Psychosis	19
Epilepsy	18
Encephalopathy of unknown aetiology[b]	17
Metabolic encephalopathy	13
Frontotemporal dementia	13
Other autoimmune encephalopathy[c]	10
Spinocerebellar degeneration	10
Corticobasal degeneration	10
Hypoxic encephalopathy	9
Dementia with Lewy bodies	8
Vascular dementia	8
Hashimoto's encephalopathy	7
Brain tumour	6
Paraneoplastic syndrome	6
Mitochondrial encephalomyopathy	5
Cerebral infarction	4
Normal pressure hydrocephalus	4
Spastic paraplegia	4
Alcohol encephalopathy	3
Central nervous system lupus	3
Frontotemporal dementia and motor neuron disease	3
Alzheimer's disease and epilepsy	2
Cerebral autosomal dominant arteriopathy with subcortical infarction and leukoencephalopathy	2
Hepatic encephalopathy	2
Multiple system atrophy	2
Progressive supranuclear palsy	2
Subacute sclerosing panencephalitis	2
Head trauma	2
Adult-onset Alexander disease	1
Adult-onset type 2 citrullinemia	1
Cervical spondylosis	1
Dementia of unknown aetiology	1
Huntington's disease	1
Hypoglycemic encephalopathy	1
Motor neuron disease	1
Multiple sclerosis	1
Spinocerebellar degeneration and motor neuron disease	1
Thyrotoxicosis	1

a Viral (including herpes simplex virus) or parasitic encephalitis.
b Encephalopathy excluding metabolic, alcohol, hepatic, hypoxic, hypoglycemic, autoimmune (CNS, Hashimoto's encephalopathy and others)-induced encephalopathy.
c Autoimmune-induced encephalopathy excluding Hashimoto's encephalopathy and CNS lupus.

Annual development of prion diseases was 82–141 cases from 1999 to 2008 (mean ± SD 108.8 ± 20.0). The incidence rate of prion diseases per million population during 1999–2008 varied from 0.64 in 1999 to 1.10 in 2006 (0.85 ± 0.16) (Fig. 1). The incidence pattern per year of sporadic Creutzfeldt–Jakob disease [0.55 in 1999 to 0.87 in 2006 (0.66 ± 0.11)] and genetic prion diseases [0.04 in 1999 to 0.20 in 2005 (0.12 ± 0.07)] resembled that of all prion diseases; however, the incidence rate of dura mater graft-associated Creutzfeldt–Jakob disease gradually decreased (0.41 ± 0.02) (Fig. 1). The annual mortality rate per million population, which was obtained by Vital Statistics of Japan, ranged from 0.88 in 1999 and 2000 to 1.59 in 2008 (1.15 ± 0.23) (Fig. 1).

Patients with prion diseases included 512 males and 710 females, and the female to male ratio of all prion diseases, sporadic Creutzfeldt–Jakob disease, dura mater graft-associated Creutzfeldt–Jakob disease and genetic prion diseases was 1.4, 1.4, 1.6 and 1.2, respectively. The age-adjusted incidence rates

Table 2 Classification of each type of prion disease according to accuracy of diagnosis

	Sporadic Creutzfeldt–Jakob disease	Variant Creutzfeldt–Jakob disease	Dura mater graft-associated Creutzfeldt–Jakob disease	Genetic prion disease	Total (%)
Definite	111	1	33	35	180 (13.6)
Probable	811	0	34	181	1026 (77.7)
Possible	97	0	13	4	114 (8.6)
Total (%)	1019 (77.2)	1 (0.1)	80 (6.1)	220 (16.7)	1320

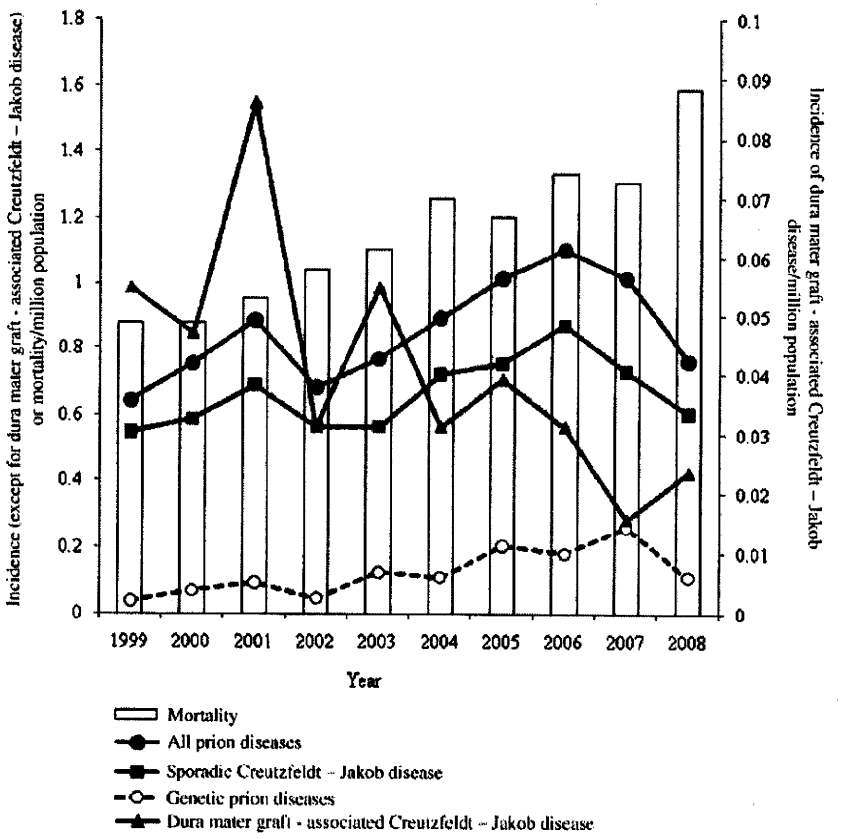

Figure 1 Based on data from 1999–2008, the crude annual incidence rates per million population of all prion diseases, sporadic Creutzfeldt–Jakob disease (CJD), dura mater graft-associated Creutzfeldt–Jakob disease and genetic prion diseases are shown. Black circles = all prion diseases; black squares = sporadic Creutzfeldt–Jakob disease; black triangles = dura mater graft-associated Creutzfeldt–Jakob disease; dotted white circles = genetic prion diseases. Crude annual mortality rate is demonstrated by white bars. The incidence rate data were obtained from this surveillance and the mortality rate data were obtained from Vital Statistics of Japan.

per million per year for females were higher than those for males in all prion diseases (male 0.79; female 0.88), sporadic Creutzfeldt–Jakob disease (male 0.62; female 0.71) and dura mater graft-associated Creutzfeldt–Jakob disease (male 0.048; female 0.074), except for genetic prion diseases (male 0.16; female 0.14).

The age at onset in all prion diseases ranged from 15 to 94 (mean ± SD 66.9 ± 11.4 years). The age at onset of dura mater graft-associated Creutzfeldt–Jakob disease was significantly younger than for sporadic Creutzfeldt–Jakob disease and genetic prion diseases ($P < 0.001$) (Table 3).

As shown in Fig. 2A, the age- and sex-specific incidence rate of all prion diseases increased with age to a peak in the eighth decade (all 3.24; male 2.95; female 3.48) for both sexes, and decreased over the age of 80 years. Sporadic Creutzfeldt–Jakob disease showed similar results, with the highest incidence rate in the eighth decade (all 2.76; male 2.51; female 2.97) (Fig. 2B). The incidence rate of dura mater graft-associated Creutzfeldt–Jakob disease showed two peaks in the fourth and eighth decades (0.03 and 0.10, respectively) (Fig. 2C). The incidence rate of male patients with dura mater graft-associated Creutzfeldt–Jakob disease also showed two peaks in the fourth and sixth decades (0.04 and 0.07, respectively), while the incidence rate of female patients with dura mater graft-associated Creutzfeldt–Jakob disease showed two peaks in the third and eighth decades (0.05 and 0.13, respectively) (Fig. 2C). The peak incidence rate of genetic prion diseases was in the ninth decade for male patients (0.62) and the eighth decade for all and female patients (0.58 and 0.69, respectively) (Fig. 2D).

In patients with genetic prion diseases, the duration between onset and akinetic mutism or death was significantly longer than in sporadic Creutzfeldt–Jakob disease and dura mater graft-associated Creutzfeldt–Jakob disease ($P < 0.001$) (Table 3).

The frequencies of each clinical sign are described in Table 3. The positive rates of PSWCs on EEG, hyperintensities on MRI and 14-3-3 protein in CSF were significantly different between sporadic Creutzfeldt–Jakob disease, dura mater graft-associated Creutzfeldt–Jakob disease and genetic prion diseases ($P < 0.001$, $P = 0.039$ and $P = 0.010$, respectively) (Table 3).

Characteristics of sporadic Creutzfeldt–Jakob disease

Genetic analyses for *PrP* were performed in 608 cases (69.6%) and the results of polymorphic codon 129 (methionine homozygotes, valine homozygotes and heterozygotes) and codon 219 (glutamic acid homozygotes, lysine homozygotes and heterozygotes) are shown in Table 3.

According to Parchi's classification based on the genotype of polymorphism at codon 129 of *PrP* and the physicochemical properties of protease K-resistant PrP, 44 patients with pathologically confirmed sporadic Creutzfeldt–Jakob disease were classified as: 25 with type MM1; 10 with type MM2, including cortical ($n = 5$), thalamic ($n = 4$) and MM2-cortical and thalamic ($n = 1$); four with type MM1+2; three with type MV2; and two with type VV2. MV1 and VV1 types were not identified (Table 4). All types were glutamic acid homozygotes at polymorphic codon 219. Among subtypes of sporadic Creutzfeldt–Jakob disease (MM1, MM2-cortical, MM2-thalamic, MV2 and VV2), age at disease onset of the MM2-thalamic subtype was significantly younger than the MM1 type or MM2-cortical and VV2 subtypes ($P = 0.0016$). In the MM1 type cases, akinetic mutism or death

Table 3 Characteristics of each type of prion disease

	Sporadic Creutzfeldt–Jakob disease ($n = 922$)	Variant Creutzfeldt–Jakob disease ($n = 1$)	Dura mater graft-associated Creutzfeldt–Jakob disease ($n = 80$)	Genetic prion disease ($n = 216$)
Male/female	381/541	1/0	30/50	97/119
Age at onset (years)[a]	68.2 ± 9.6 (32–94)	48	56.5 ± 16.0 (15–80)	65.5 ± 13.9 (15–93)
Duration[b]	4.6 ± 7.9 (0–168)	23	5.7 ± 4.3 (1–16)	15.5 ± 21.4 (0–120)
Cerebellar signs (%)	467/911 (51)	1/1 (100)	61/79 (77)	111/212 (52)
Psychiatric symptoms (%)	565/901 (63)	1/1 (100)	47/75 (63)	115/208 (55)
Dementia (%)	916/919 (100)	1/1 (100)	78/80 (98)	198/213 (93)
Visual disturbance (%)	385/907 (42)	0/1 (0)	33/77 (43)	36/205 (18)
Myoclonus (%)	867/919 (94)	1/1 (100)	69/79 (87)	121/210 (58)
Extrapyramidal signs (%)	582/906 (64)	0/1 (0)	52/79 (66)	112/210 (53)
Pyramidal signs (%)	618/909 (68)	1/1 (100)	56/78 (72)	112/212 (53)
Codon 129 polymorphism	MM 552; MV 14; VV 4	MM	MM 52; MV 2	MM 168; MV 32
Codon 219 polymorphism	EE 561; EK 3	EE	EE 49; EK 2	EE 189; EK 3; KK 1
PSWCs on EEG (%)	889/920 (97)	1/1 (100)	53/80 (66)	77/212 (36)
Hyperintensities on MRI (%)	719/874 (82)	1/1 (100)	41/60 (68)	159/201 (79)
Positive 14-3-3 protein (%)	384/439 (87)	1/1 (100)	24/29 (83)	75/98 (77)

a Age at onset is expressed as the mean ± SD (range) years.
b Duration between the onset and akinetic mutism or death without akinetic mutism. Duration is expressed as the mean ± SD (range) months.
EE = glutamic acid homozygosity; EK = glutamic acid/lysine heterozygosity; KK = lysine homozygosity; MM = methionine homozygosity; MV = methionine/valine heterozygosity; VV = valine homozygosity.

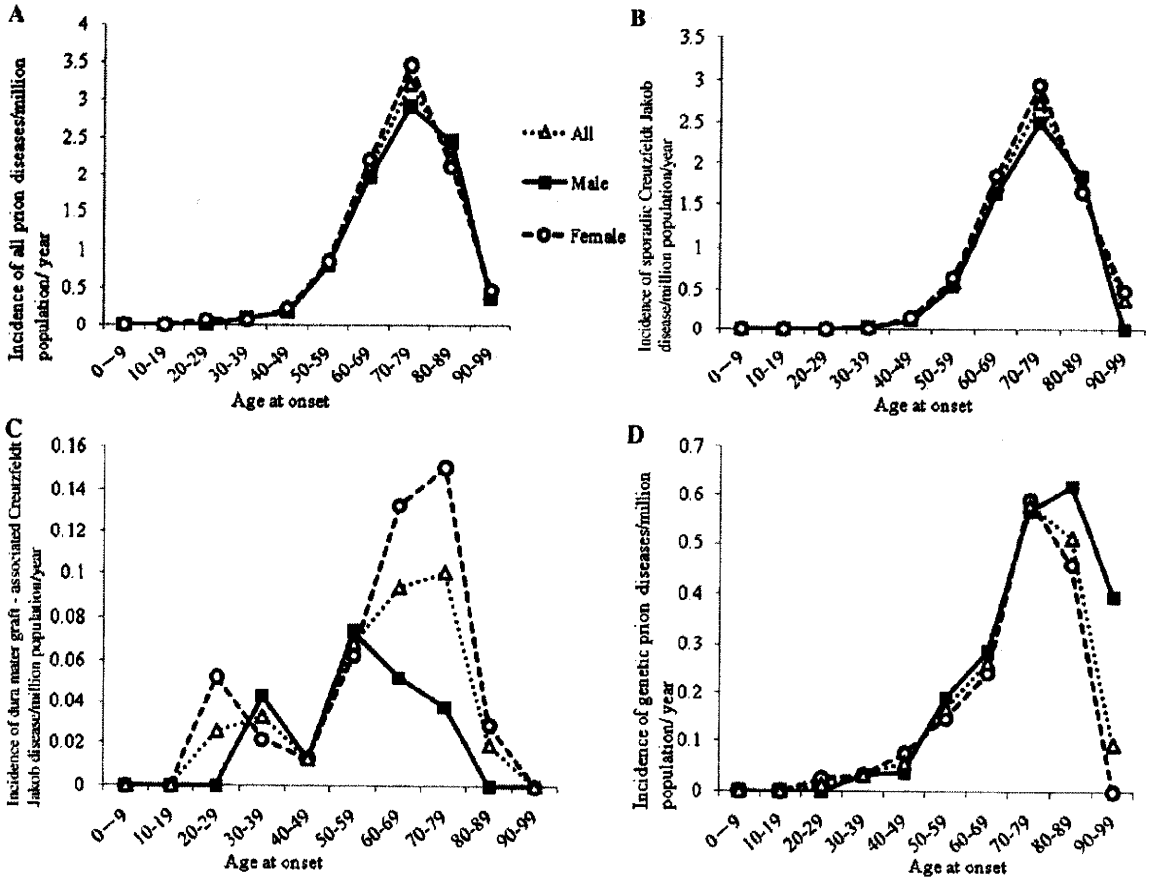

Figure 2 Based on data from 1999–2008, age- and sex-specific annual incidence per million population of all prion diseases (**A**), sporadic Creutzfeldt–Jakob disease (**B**), dura mater graft-associated Creutzfeldt–Jakob disease (**C**), and genetic prion diseases (**D**) is shown. Dotted white triangles = all patients; black squares = male patients; dashed white circles = female patients.

occurred significantly earlier than in MM2-cortical, MM2-thalamic and MV2 subtypes ($P<0.001$). Frequencies of positive PSWCs were lower in MM2-cortical, MM2-thalamic, MV2 and VV2 subtypes compared with the MM1 type. The positive rate of CSF 14-3-3 protein in the MM1 type was higher than in MM2-cortical, MM2-thalamic and MV2 subtypes. Hyperintensities on MRI were identified in all but patients with the MM2-thalamic subtype.

Characteristics of variant Creutzfeldt–Jakob disease

Only one patient with a history of a short stay in the UK, France and other European countries developed variant Creutzfeldt–Jakob disease; this case has already been reported (Yamada, 2006). Although the clinical features in the early stage were compatible with variant Creutzfeldt–Jakob disease (Will *et al.*, 2004), the patient showed PSWCs on EEG in the late stage, leading to the diagnosis of probable sporadic Creutzfeldt–Jakob disease. At polymorphic codons 129 and 219 the patient was homozygotic for methionine and glutamic acid, respectively. The patient developed akinetic mutism at 23 months and died 42 months after onset; autopsy confirmed the diagnosis of variant Creutzfeldt–Jakob disease (Table 3).

Characteristics of dura mater graft-associated Creutzfeldt–Jakob disease

Besides the 80 patients with dura mater graft-associated Creutzfeldt–Jakob disease identified by this surveillance system, 58 patients with dura mater graft-associated Creutzfeldt–Jakob disease had already been reported by previous surveillance systems (Yamada *et al.*, 2009); therefore, the total number of dura mater graft-associated Creutzfeldt–Jakob disease patients was 138. The source of cadaveric dura mater was Lyodura® (B. Braun, Germany) in all dura mater graft-associated Creutzfeldt–Jakob disease cases in which the brand name could be identified.

Table 4 Characteristics of each subtype of sporadic Creutzfeldt–Jakob disease

	MM1 ($n=25$)	MM1+2 ($n=4$)	MM2-cortical ($n=5$)	MM2-thalamic ($n=4$)	MM2-cortical and thalamic ($n=1$)	MV2 ($n=3$)	VV2 ($n=2$)
Male/female	11/14	1/3	2/3	3/1	1/0	3/0	1/1
Age at onset[a]	67.2 ± 5.5 (57–77)	66.3 ± 4.8 (62–73)	66.8 ± 7.3 (57–74)	52.8 ± 8.3 (43–61)	65	62.0 ± 5.3 (58–68)	72 (69–75)
Duration[b]	3.1 ± 2.7 (0–14)	7.5 ± 5.4 (3–14)	24.7 ± 15.1 (10–50)	18.5 ± 6.7 (13–28)	11	26.5 (12–41)	6
Codon 219 polymorphism	EE 23	EE 3	EE 5	EE 3	EE	EE 3	EE 2
PSWCs on EEG (%)	23/25 (92)	4/4 (100)	2/4 (40)	0/4 (0)	0/1 (0)	0/3 (0)	0/2 (0)
Hyperintensities on MRI (%)	25/25 (100)	4/4 (100)	5/5 (100)	0/4 (0)	1/1 (100)	3/3 (100)	2/2 (100)
Positive 14-3-3 protein (%)	15/16 (94)	3/4 (75)	2/5 (40)	1/3 (33)	0/1 (0)	0/1 (0)	2/2 (100)

a Age at onset is expressed as the mean ± SD (range) years.
b Duration between the onset and akinetic mutism or death without akinetic mutism. Duration is expressed as the mean ± SD (range) months.

Table 5 Medical conditions leading to use of dura mater grafts

Medical conditions	No. of cases
Meningioma	29
Hemifacial spasm	19
Acoustic neurinoma	17
Subarachonoid haemorrhage	11
Cerebral/cerebellar haemorrhage	8
Arteriovenous malformation	7
Trigeminal neuralgia	7
Brain aneurysm	6
Epidural/subdural haematoma	6
Trauma	6
Arnold-Chiari malformation	5
Ependymoma	2
Epidermoid	2
Glioma	2
Hemangioblastoma	2
Spinal cord tumour	2
Arachonoid cyst	1
Osteoma	1
Ossification of the posterior longitudinal ligament	1
Pituitary adenoma	1
Teratoma	1
Brain tumour with unknown details	2

The medical conditions for which dura mater grafts were used in neurosurgery included meningioma (21.0%), hemifacial spasm (13.8%) and acoustic neurinoma (12.3%) (Table 5). The proportion of non-life-threatening conditions, such as hemifacial spasm (13.8%) and trigeminal neuralgia (5%), were relatively high (Table 5). Dura mater grafts were implanted during 1975–93, and most patients (112 cases, 81.2%) received them during 1983–87 (Fig. 3A); in May 1987 the procedures for the collection and processing of grafts were revised by the company (Sato *et al.*, 1997). It was reported that one of the patients with dura mater graft-associated Creutzfeldt–Jakob disease, who received dura mater grafts after May 1987, received a graft that had been produced before May 1987. The incubation period (i.e. duration from implantation of dura mater grafts to dura mater graft-associated Creutzfeldt–Jakob disease onset) ranged from 1 to 30 years (mean ± SD 11.8 ± 5.5 years) (Fig. 3B). The year of disease onset ranged from 1985 to 2008, and many patients (83 cases, 60.1%) developed dura mater graft-associated Creutzfeldt–Jakob disease during 1993–2001, with a peak in 1995 (Fig. 3C).

Genetic analyses for *PrP* were performed in 58 cases (73.1%). The polymorphic *PrP* codon 129 included 52 methionine homozygotes (96.3%) and two heterozygotes (3.7%), and for codon 219, 49 glutamic acid homozygotes (96.1%) and two heterozygotes (3.9%) (Table 3).

Among 33 patients with definite dura mater graft-associated Creutzfeldt–Jakob disease, 29 patients had sufficient pathological data to be categorized as either plaque type ($n=14$, 48%) or non-plaque type ($n=15$, 52%).

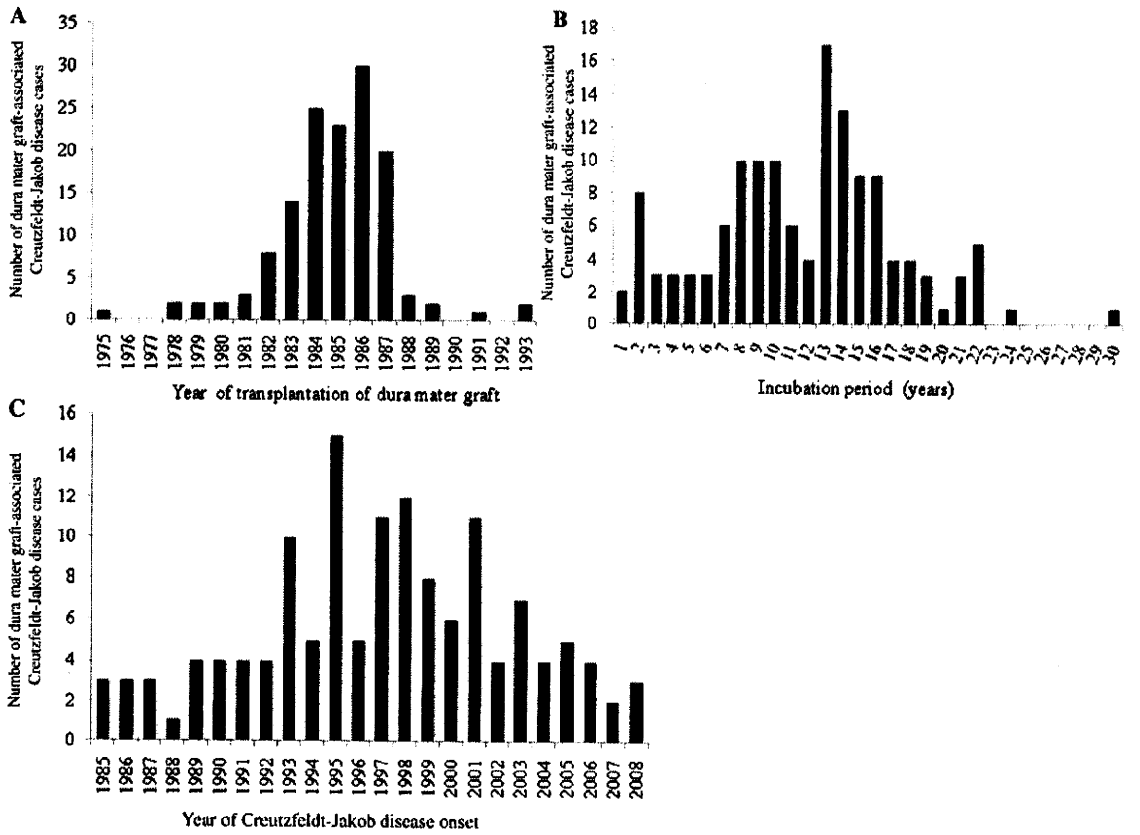

Figure 3 The time when cadaveric dura mater grafts were implanted is shown by year, with black bars indicating patients with dura mater graft-associated Creutzfeldt–Jakob disease (**A**). The incubation period (i.e. duration from implantation of dura mater grafts to onset of dura mater graft-associated Creutzfeldt–Jakob disease) is shown by year, with black bars indicating patients with dura mater graft-associated Creutzfeldt–Jakob disease (**B**). The year when dura mater graft-associated Creutzfeldt–Jakob disease developed in patients is shown by black bars indicating patients with dura mater graft-associated Creutzfeldt–Jakob disease (**C**).

Characteristics of genetic prion diseases

The distribution and frequencies of *PrP* mutations associated with genetic prion diseases in Japan are shown in Table 6. The most common mutation was V180I, followed by P102L, E200K, M232R and P105L. The characteristics associated with the mutations are shown in Table 7. The characteristics of relatively frequent mutations in Japan (P102L, P105L, V180I, E200K and M232R) were as follows: patients with P102L, P105L and E200K showed relatively high penetrance (Table 7), whereas only 2.2% of patients with V180I mutation and no patients with M232R mutation had a positive family history (Table 7).

P102L and P105L cases showed onset at a relatively young age and a Gerstmann–Sträussler–Scheinker disease phenotype with slow progression, while V180I cases presented with onset in old age and with slow progression in spite of the Creutzfeldt–Jakob disease type pathology (Mutsukura *et al.*, 2009) (Table 7). Thirty-one M232R patients with sufficient clinical data were classified into 19 with rapid type and 12 with slow type.

P102L and P105L showed low positive rates in PSWCs on EEG and hyperintensities on MRI. V180I and the slow type of M232R presented with a low positive rate of PSWCs on EEG, but a high positive rate of hyperintensities on MRI.

Discussion

This study revealed the epidemiological and clinical characteristics of prion diseases in Japan over a 10-year period. Nationwide surveillance data of prion diseases have been reported from European countries, Australia and the USA (Horan *et al.*, 2004; Sanchez-Valle *et al.*, 2004; Ladogana *et al.*, 2005; de Pedro-Cuesta *et al.*, 2006; Van Everbroeck *et al.*, 2006; Heinemann *et al.*, 2007; Klug *et al.*, 2009; Holman *et al.*, 2010). Although a study of Chinese patients with prion diseases has been reported (Shi *et al.*, 2008), it did not accurately reflect the incidence rate in China, as the number of patients with prion diseases was quite small compared with that estimated for the population in China.

Table 6 Comparison of the distribution in genetic prion disease between Japan and EUROCJD

	Japan (*n*=216) (%)	EUROCJD[a] (*n*=425) (%)
Insertion	3 (1.4)	42 (9.9)
P102L	39 (18.1)	24 (5.6)
P105L	5 (2.3)	0 (0)
A117V-129V	0 (0)	12 (2.8)
D178N-129M	3 (1.4)	64 (15.1)
D178N-129V	1 (0.5)	16 (3.8)
V180I	89 (41.2)	1 (0.2)
E200K	37 (17.1)	175 (41.2)
V203I	2 (0.9)	5 (1.2)
R208H	1 (0.5)	2 (0.5)
V210I	0 (0)	69 (16.2)
M232R	33 (15.3)	0 (0)
V180I+M232R	1 (0.5)	0 (0)
Other mutations	0 (0)	15 (3.5)

a European Creutzfeldt–Jakob Disease Surveillance Network; Kovacs *et al.*, 2005.

Our study is therefore the largest report of prospective prion disease surveillance from Asia.

Incidence rate of prion diseases

The crude annual mortality rate per million of prion diseases in Japan was 0.89–1.58 (mean 1.18), which was obtained from Vital Statistics of Japan and is similar to that in European countries, Australia, Canada and the USA (1.0–1.5 per million) (Ladogana *et al.*, 2005; Klug *et al.*, 2009; Holman *et al.*, 2010). On the other hand, the annual incidence rate of prion diseases per million population in Japan obtained by our surveillance was 0.65–1.10 (mean 0.85), which was lower than the mortality rate obtained by Vital Statistics of Japan, because our surveillance rate was not 100%. The annual incidence rate of sporadic Creutzfeldt–Jakob disease in Japan was 0.55–0.87 per million (mean 0.66), which was slightly lower than in Germany (0.8–1.6) and in European countries, Australia and Canada (1.39 as overall annual mortality rate) (Ladogana *et al.*, 2005; Heinemann *et al.*, 2007). The reasons for the lower incidence rate of sporadic Creutzfeldt–Jakob disease in Japan may be explained by the lower autopsy rate in Japan compared with other western countries, and the limited sensitivity of the diagnostic criteria by Masters *et al.* (1979) for probable sporadic Creutzfeldt–Jakob disease. When possible sporadic Creutzfeldt–Jakob disease cases were included in the number of sporadic Creutzfeldt–Jakob disease cases, the annual incidence rate per million increased to 0.57–0.95 (mean 0.73), but it was still lower than those of other western countries.

Interestingly, in Japan, female predominance was identified in age-adjusted incidence rates of prion diseases, sporadic Creutzfeldt–Jakob disease, and dura mater graft-associated Creutzfeldt–Jakob disease, but not for genetic prion diseases. An excess of females has been reported for Creutzfeldt–Jakob disease, sporadic Creutzfeldt–Jakob disease or genetic cases (Collins *et al.*,

Table 7 Characteristics of genetic prion diseases

	Insertion (*n*=3)	P102L (*n*=39)	P105L (*n*=5)	D178N-129M (*n*=3)	D178N-129V (*n*=1)	V180I (*n*=89)	E200K (*n*=37)	V203I (*n*=2)	R208H (*n*=1)	M232R (*n*=33)	V180I+M232R (*n*=1)
Male/female	2/1	16/23	4/1	2/1	1/0	35/54	15/22	2/0	0/1	18/15	0/1
Age at onset[a]	49.5±21.7 (26–55)	54.0±12.4 (22–75)	41.6±8.0 (31–51)	52.3±5.7 (46–57)	74	76.1±7.4 (44–93)	58.5±9.8 (31–77)	73	74	64.2±12.5 (15–81)	74
Positive family history (%)	1 (33)	29 (74)	4 (80)	None	None	2 (2)	17 (46)	None	None	None	None
Duration[b]	20.0±21.4 (3–44)	36.7±30.1 (3–96)	99.7±23.5 (74–120)	10.7±3.2 (7–13)	24	13.3±10.9 (1–58)	3.9±3.6 (1–14)	5 (4–6)	3	8.0±8.7 (0–32)	1
Codon 129 polymorphism	MM 2	MM 29; MV 3	MV 4	MM 3	MV 1	MM 65; MV 22	MM 34	MM 2	MM 1	MM 30; MV 2	MM 1
Codon 219 polymorphism	EE 1; KK 1	EE 31; EK 1	EE 4	EE 3	EE 1	EE 81	EE 33; EK 1	EE 2	EE 1	EE 31; EK 1	EE 1
PSWCs on EEG (%)	2/3 (67)	7/37 (19)	0/5 (0)	0/3 (0)	0/1 (0)	10/88 (11)	34/37 (92)	2/2 (100)	1/1 (100)	20/32 (63)	1/1 (100)
Hyperintensities on MRI (%)	1/2 (50)	14/36 (39)	0/5 (0)	0/3 (0)	0/1 (0)	84/84 (100)	31/35 (89)	2/2 (100)	1/1 (100)	26/31 (84)	0/1 (0)
Positive 14-3-3 protein (%)	0/1 (0)	6/10 (60)	1/2 (50)	1/1 (100)	1/1 (100)	35/45 (78)	11/12 (92)	1/1 (100)	1/1 (100)	18/23 (78)	0/1 (0)

EE = glutamic acid homozygosity; EK = glutamic acid/lysine heterozygosity; KK = lysine homozygosity; MM = methionine homozygosity; MV = methionine/valine heterozygosity; PSWCs = periodic synchronous wave complexes; VV = valine homozygosity.
a Age at onset is expressed as the mean ± SD (range) years.
b Duration between the onset and akinetic mutism or death without akinetic mutism. Duration is expressed as the mean ± SD (range) months.

2002, 2006; Kovács *et al.*, 2005; Holman *et al.*, 2010); however, the average age-adjusted incidence rate of Creutzfeldt–Jakob disease was reported to be similar for males and females in Australia (Collins *et al.*, 2002) and higher for males than for females in the USA (Holman *et al.*, 2010). Further data corrected by the age distribution of gender in the general population of each country are essential to clarify gender difference.

The age- and sex-specific incidence rate of sporadic Creutzfeldt–Jakob disease in Japan was similar to that of sporadic Creutzfeldt–Jakob disease in European countries, Australia and Canada (Ladogana *et al.*, 2005; Heinemann *et al.*, 2007), showing a decreased incidence rate over the age of 80 years. The reason for this remains unknown and requires further study. The age- and sex-specific incidence rate of patients with dura mater graft-associated Creutzfeldt–Jakob disease showed two peaks, reflecting two peaks in the age at dura mater transplantation (male, second and fifth decade; female, second and sixth decade) (data not shown). The incidence pattern of genetic prion diseases peaked in old age, similar to sporadic Creutzfeldt–Jakob disease, and seemed to be influenced by onset in old age in a high proportion of patients with the V180I mutation.

Types of prion diseases

The proportions of sporadic Creutzfeldt–Jakob disease and genetic prion diseases were almost identical to those in European countries, except for Slovakia, in which the percentage of patients with genetic prion diseases was 70% (Ladogana *et al.*, 2005). The proportion of iatrogenic Creutzfeldt–Jakob disease was relatively high in Japan compared with other European countries because of the large number of patients with dura mater graft-associated Creutzfeldt–Jakob disease. Of the 196 (62.7%) worldwide dura mater graft-associated Creutzfeldt–Jakob disease cases, 123 had been identified in Japan up to 2006 (Brown *et al.*, 2006). In France, the proportion of iatrogenic Creutzfeldt–Jakob disease was also high (8.7%) (de Pedro-Cuesta *et al.*, 2006), but most iatrogenic Creutzfeldt–Jakob disease cases were induced by contaminated human growth hormone (Brown *et al.*, 2006). Worldwide, contaminated human growth hormone-associated Creutzfeldt–Jakob disease was the most common iatrogenic Creutzfeldt–Jakob disease, except for dura mater graft-associated Creutzfeldt–Jakob disease (Brown *et al.*, 2006), although there were no cases of human growth hormone-associated Creutzfeldt–Jakob disease in Japan. Although there was only one case of variant Creutzfeldt–Jakob disease in the past 10 years in Japan, the number of variant Creutzfeldt–Jakob disease cases was 212 cases worldwide, in particular 172 (81.3%) in the UK and 25 (11.8%) in France, up to March 2010 (NCJDSU) (http://www.cjd.ed.ac.uk/vcjdworld.htm).

PrP polymorphisms in prion diseases

The genotype distribution at codon 129 of *PrP* in sporadic Creutzfeldt–Jakob disease in Japan revealed a higher proportion of methionine homozygotes (96.8%) than in European countries, Australia and Canada (67.2%) (Ladogana *et al.*, 2005), whereas the proportion of methionine homozygotes at codon 129 in sporadic Creutzfeldt–Jakob disease was 100% (150/150) in Korea (Jeong *et al.*, 2005) and 97.0 % (131/135) in China (Shi *et al.*, 2008), similar to Japan.

The general Japanese population also presented with a higher frequency of codon 129 homozygosity (methionine homozygotes: 0.92, heterozygotes: 0.08, valine homozygotes: 0) than European countries (methionine homozygotes: 0.37–0.49, heterozygotes: 0.42–0.49, valine homozygotes: 0.08–0.15) (Collinge *et al.*, 1991; Doh-ura *et al.*, 1991; Zimmermann *et al.*, 1999; Nurmi *et al.*, 2003; Mitrová *et al.*, 2005; Georgsson *et al.*, 2006; Dyrbye *et al.*, 2008). The proportion of methionine homozygotes at codon 129 in the general population was 94.3% (499/529) in Korea (Jeong *et al.*, 2004) and 97.6% (200/205) among Han Chinese (Yu *et al.*, 2004), also similar to Japan.

Genetic predisposition to sporadic Creutzfeldt–Jakob disease in codon 129 homozygosity (methionine homozygotes or valine homozygotes) was revealed in the UK (Palmer *et al.*, 1991), but this predisposition was not previously identified in a small number of Japanese sporadic Creutzfeldt–Jakob disease patients ($n=21$; methionine homozygotes or valine homozygotes: 0.95, heterozygotes: 0.05) because of the high frequency of methionine homozygotes at codon 129 in the general Japanese population (Doh-ura *et al.*, 1991). Using data on codon 129 polymorphisms ($n=645$; methionine homozygotes: 0.93, heterozygotes: 0.07, valine homozygotes: 0; M allele: 0.97, V allele: 0.03) in the general Japanese population obtained from combining previous data (Doh-ura *et al.*, 1991; Ohkubo *et al.*, 2003) as a control, we assessed whether homozygosity, methionine homozygosity or the M allele at codon 129 was associated with sporadic Creutzfeldt–Jakob disease in Japan, and found a significant association ($P<0.001$, $P=0.004$ and $P=0.019$, respectively). This is the first report showing that codon 129 homozygosity is a risk for sporadic Creutzfeldt–Jakob disease in Asia, as reported in western countries. In addition, methionine homozygosity and the M allele were not associated with sporadic Creutzfeldt–Jakob disease in the UK (Palmer *et al.*, 1991). In dura mater graft-associated Creutzfeldt–Jakob disease, neither homozygosity (methionine homozygotes or valine homozygotes: 0.96), methionine homozygosity (0.96) nor the M allele (0.98) at codon 129 were significantly different from the general Japanese population. Genetic prion diseases had a significantly higher proportion of codon 129 heterozygosity and the V allele than the general population (both $P<0.001$). This seemed to be related to the higher proportion of codon 129 heterozygosity in V180I cases (methionine homozygotes: 0.75, heterozygotes: 0.25), which is the most common genetic prion disease in Japan, although the V180I mutation was located on the allele with methionine at codon 129 in all cases investigated.

It was previously reported that heterozygosity at codon 219 was found in the general Japanese population (glutamic acid homozygotes: 0.88, heterozygotes: 0.12), while the K allele was not found in 85 Japanese patients with sporadic Creutzfeldt–Jakob disease (Shibuya *et al.*, 1998). The frequencies of the K allele (0.0027) and heterozygous genotype (heterozygotes: 0.0053) at codon 219 in sporadic Creutzfeldt–Jakob disease patients in this study were significantly lower than in the general Japanese population